Surface optical phonons in ionic crystals

V. V. Bryksin, D. N. Mirlin, and Yu. A. Firsov

A. F. Ioffe Physico-technical Institute, USSR Academy of Sciences
Usp. Fiz. Nauk **113**, 29–67 (May 1974)

The review is devoted to the present status of theory and experiment in the region of surface optical oscillation (SO) in ionic crystals. Results are presented of a phenomenological analysis of the SO, and a microscopic theory of SO is developed. Results of recent experiments on the observation and investigation of SO by the methods of electron and infrared spectroscopy are reported and analyzed. The conclusion deals briefly with other types of surface excitations (surface plasmons, magnons, and excitons.)

CONTENTS

I. INTRODUCTION

The influence of the surface on the elementary-excitation spectrum has been under study for many years. Calculation of the spectra in crystals is usually based on the use of cyclic boundary conditions of the Born-von Karman type[1]. The presence of a surface disturbs the translational symmetry of the crystal, and leads in final analysis to the appearance of surface states[1]. The presence of the surface leads, on the one hand, to a weak deformation (in terms of the parameter S/V, where S and V are the surface area and the volume of the crystal) of the spectrum of the volume excitations obtained with the aid of the cyclic boundary conditions, and on the other hand to the appearance in the spectrum of surface excitations whose number is small in comparison with the number of volume excitations, in terms of the same parameter S/V. These surface states appear in the spectra of electrons (Tamm levels), phonons, plasmons, excitons, magnons, etc.

A very important role in the behavior (and in the method of description) of surface excitations is played by their characteristic dimension, which is the distance over which the amplitude decreases with decreasing distance from the surface. If this decrease is slow enough, over distances much larger than microscopic (for example, the characteristic microscopic dimension for phonons is the lattice constant a), then such excitations can be described phenomenologically[2]. We shall arbitrarily call them surface oscillations of type I—SO-I (this terminology was first used for surface phonons). Surface excitations whose amplitude decreases rapidly, over distances comparable with the microscopic ones, will be called surface oscillations of type II (SO-II). The SO-II can be investigated only within the framework of the microscopic theory, which was first formulated in[3] (see also[4]).

One form of SO-I are Rayleigh waves, i.e., surface oscillations in acoustic phonon modes, and have been known for a very long time. Rayleigh waves are described theoretically within the framework of elasticity theory (see, e.g.,[5]). Their amplitude decreases exponentially away from the surface over distances on the order of the wavelength, which can appreciably exceed the lattice constant, and this indeed is the reason for the success of the phenomenological method. Rayleigh waves have by now been sufficiently well investigated both theoretically and experimentally (see, e.g.,[6,7]) and have found rather extensive practical applications.

If a dipole moment, and consequently also an electric field, is produced in the course of type-I oscillations, then it is obvious that the phenomenological solution of the SO-I problem must be sought with the aid of Maxwell's equations. The first such approach was used to develop a theory of surface plasmons in metals[8,9][2]. It is obvious that SO-I can arise also in the case of lattice vibrations of an ionic crystal. Inasmuch as surface phonon levels (bands) are component parts of the spectrum of the natural oscillations of the macroscopic dipole moment, it follows that they can also be obtained from Maxwell's equations[11-14]. In the theory of surface excitons, these waves are called surface Coulomb excitons[2,15].

Ordinary electrodynamics without allowance for spatial dispersion yields only surface oscillations corresponding to a very slow damping of the amplitudes with increasing distance from the surface. The dependence of the frequency ω_S^I of SO-I on their wavelength λ is determined in this approximation by two dimensionless parameters, L/λ and $c/\omega_{TO}\lambda$, where L is the characteristic linear dimension of the sample and ω_{TO} is the frequency of the transverse optical phonon[12-14]. The dependence of ω_S^I on the third dimensionless parameter a/λ cannot be obtained in this approximation. On the other hand, the calculation of the corrections to the spectrum in terms of the parameter a/λ, at $a/\lambda \ll 1$, within the framework of electrody-

namics with allowance for weak spatial dispersion, entails certain difficulties (see below), and this problem has been solved so far only within the framework of the microscopic approach, in which account is taken not only of the short-range inter-ion forces, but also the Coulomb long-range forces[16,17].

A method that makes it possible to determine surface oscillations on the basis of a microscopic theory, when the effective radius of the interatomic forces is small (on the order of several lattice constants), was first formulated in[3] (see also[4,7]) and was called the Green's-function method. This method is used successfully in the calculations of the surface on local oscillations in homopolar crystals. A review of studies of this type can be found in[7].

The first attempt to calculate the surface-oscillation spectrum within the framework of a microscopic theory for ionic crystals, where long-range Coulomb forces are significant, was made in[18]. However, only the case $\lambda \to \infty$ was investigated there. A microscopic study of surface oscillations in ionic crystals at arbitrary λ was carried out in[16,17,19]. A unified scheme for describing SO-I and SO-II, proposed in[16,17], has made it possible to generalize the Green's-function method to include the case of long-range forces.

Although the fraction of the surface oscillations is small in comparison with the volume oscillations in crystals having macroscopic dimensions, the ratio of their contribution to the experimentally measured quantities to the contribution due to the volume oscillations turns out as a rule to be of the order of λ_0/L (λ_0 is the wavelength of the "probing" radiation—electrons or light), which is close to unity even at microscopic sample dimensions. Therefore the surface oscillations in ionic crystals can be relatively easily observed in experiment. An intensive experimental study is presently being made of surface phonons in ionic crystals by electron-beam diffraction and infrared spectroscopy methods.

Surface optical phonons were observed in a study[20] of the passage of fast electrons through an LiF plate. In optical experiments, SO-I were first observed in powders[21-23] and later in plate[24]. A detailed review of these and other experimental studies is given below.

2. PHENOMENOLOGICAL METHOD OF CALCULATING SURFACE OSCILLATIONS IN IONIC CRYSTALS

It was noted in the introduction that SO-I constitute a certain fraction ($\sim S/V$) of the natural oscillations of the macroscopic dipole moment of the sample, and are accompanied by the onset of a macroscopic electric field, so that they can be described with the aid of Maxwell's equations[2,11-15,25-34]. Oscillations of the SO-I type are produced not only in dielectrics of the ionic type, but also in all other crystals in which long-range forces are present. These are surface plasmons in metals and semiconductors (see, e.g.,[8-10,35,36]) or surface excitons in semiconductors and in molecular crystals (see, e.g.,[2,15,37,38]), surface magnons in ferromagnets and antiferromagnets[39,40], etc. The concept of the unity of all these phenomena is most clearly developed in the monograph[2], where all the surface excitations of the SO-I type are called surface excitons. The distinguishing feature of any particular surface excitation is manifest only in the concrete form of the dielectric constant of the crystal $\epsilon(\omega)$ (or its magnetic permeability $\mu(\omega)$). Since the basic dispersion equations for surface excitations can be expressed in terms of $\epsilon(\omega)$, the problem of finding the form of the dispersion curve for a particular type of surface excitations reduces only to a substitution of the required form of $\epsilon(\omega)$ in the dispersion relations and to solving this equation with respect to ω. As already noted, it is possible to determine in this manner ω_S^I for arbitrary L/λ, $c/\omega_{TO}\lambda$, but $a/\lambda \to 0$.

Detailed phenomenological calculations of the SO-I spectra as applied to ionic crystals were carried out in[12-14,30-34]. Since these calculations are described in sufficient detail in the review[33], we present here only the main ideas of the calculations and the final results.

We assume henceforth that the crystal is isotropic and that its magnetic susceptibility is equal to unity (some results for anisotropic crystals are given below). The electric and magnetic fields **E** and **H** inside the crystal are then described by the Helmholtz vector equations

$$\left(\Delta + \varepsilon(\omega)\frac{\omega^2}{c^2}\right)\mathbf{E} = \left(\Delta + \varepsilon(\omega)\frac{\omega^2}{c^2}\right)\mathbf{H} = 0. \tag{2.1}$$

We assume for simplicity that the dielectric constant of the surrounding medium is $\epsilon_M = \text{const}(\omega)$ in the frequency region of interest to us. Outside the crystal, the fields $\mathbf{E}_M$ and $\mathbf{H}_M$ are described by the equations

$$\left(\Delta + \varepsilon_M\frac{\omega^2}{c^2}\right)\mathbf{E}_M = \left(\Delta + \varepsilon_M\frac{\omega^2}{c^2}\right)\mathbf{H}_M = 0. \tag{2.2}$$

To determine the spectrum of the natural oscillations from (2.1) and (2.2), one uses the condition that no electromagnetic wave is incident on the crystal, the usual boundary conditions for the conservation of the normal component of the induction **D** and the tangential component of the field **E**, and also the continuity condition for **H**.

The variables in (2.1) and (2.2) can be separated in six coordinate systems[41]: rectangular, spherical, circular-cylindrical, parabolic-cylindrical, elliptic-cylindrical, and conical. By now, the solutions of (2.1) and (2.2) have been investigated in the rectangular, spherical and circular-cylindrical coordinate systems, so that dispersion relations were obtained for SO-I in a plate[12-14], a sphere[31], and a cylinder[32]. In addition, SO-I in a wedge were investigated in[34] without taking retardation into account.

Since **E** and **H** are solenoidal vectors, the solution of Eqs. (2.1) and (2.2) can be expressed in the form of a superposition of two solutions **M** and **N**:

$$\mathbf{M} = \text{rot}(\mathbf{a}w\Psi), \quad \mathbf{N} = \text{rot rot}(\mathbf{a}w\Psi), \tag{2.3}$$

where Ψ is the solution of the scalar Helmholtz equation

$$(\Delta + \lambda^2)\Psi = 0, \quad \lambda^2 = \begin{cases} \varepsilon(\omega)\omega^2/c^2 \text{ in the crystal,} \\ \varepsilon_M\omega^2/c^2 \text{ outside the crystal.} \end{cases} \tag{2.4}$$

For rectangular and cylindrical coordinates we have in (2.3) $\mathbf{a} = \mathbf{e}_z$ and $w = 1$, and for spherical coordinates we have $\mathbf{a} = \mathbf{e}_r$ and $w = r$ ($\mathbf{e}$ is a unit vector).

The modes for which $\mathbf{E} \sim \mathbf{N}$ and $\mathbf{H} \sim \mathbf{M}$ are called electric (E modes), and those with $\mathbf{E} \sim \mathbf{M}$ and $\mathbf{H} \sim \mathbf{N}$ are called magnetic (H modes). We present here the results of the calculations for a plate, sphere, and cylinder.

a) Plate[12-14]. We direct the z axis along the normal

to the surface of a plate of thickness L, and place the origin at the center of the plate. We use periodic boundary conditions in the (x, y) plane, by virtue of which the solution for (2.4) is

$$\Psi = \exp(iq_x x)\begin{cases} a_1 \exp(-\varkappa_0 z), & z > \frac{L}{2}, \\ a_2 \exp(-\varkappa z) + a_3 \exp(\varkappa z), & \frac{L}{2} > z > -\frac{L}{2}, \\ a_4 \exp(\varkappa_0 z), & z < -\frac{L}{2}; \end{cases} \quad (2.5)$$

we have introduced here a two-dimensional wave vector $\mathbf{q}_\perp$ lying in the (x, y) plane parallel to the surface, while the x axis is directed along $\mathbf{q}_\perp$, so that $q_y = 0$,

$$\varkappa_0 = \left(q_x^2 - \frac{\omega^2}{c^2}\varepsilon_M\right)^{1/2}, \quad \varkappa = \left(q_x^2 - \frac{\omega^2}{c^2}\varepsilon(\omega)\right)^{1/2}. \quad (2.6)$$

The coefficients a_i in (2.5) must be determined from the boundary conditions.

1) Electric modes (E ~ M, H ~ N). These modes for a plate are also called p-polarized, since E lies in the (x, z) plane. Using (2.3) and (2.5), we set up four homogeneous equations for a_i. Solving the corresponding characteristic equation, we obtain the following dispersion relations for the frequencies of the natural oscillations:

$$\frac{\varepsilon(\omega)}{\varepsilon_M} = -\frac{\varkappa}{\varkappa_0}\operatorname{th}\left(\frac{\varkappa L}{2}\right), \quad (2.7a)$$

$$\frac{\varepsilon(\omega)}{\varepsilon_M} = -\frac{\varkappa}{\varkappa_0}\operatorname{cth}\left(\frac{\varkappa L}{2}\right). \quad (2.7b)$$

The dipole moment (and the electric field) produced inside the plate in the case of E modes, depends on the coordinates in the following manner:

$$P_z \sim \operatorname{ch}(\varkappa z)\exp(iq_x x), \quad P_x \sim \operatorname{sh}(\varkappa z)\exp(iq_x x), \quad (2.8a)$$

$$P_z \sim \operatorname{sh}(\varkappa z)\exp(iq_x x), \quad P_x \sim \operatorname{ch}(\varkappa z)\exp(iq_x x), \quad (2.8b)$$

and outside in the plate

$$E_x, E_z \sim \exp(iq_x x \pm \varkappa_0 z). \quad (2.9)$$

2) Magnetic modes (E ~ N, H ~ M) (or s-polarized modes (H in the (x, z) plane)). The dispersion relations for these modes are

$$1 = -\frac{\varkappa}{\varkappa_0}\operatorname{th}\left(\frac{\varkappa L}{2}\right), \quad (2.10a)$$

$$1 = -\frac{\varkappa}{\varkappa_0}\operatorname{cth}\left(\frac{\varkappa L}{2}\right), \quad (2.10b)$$

The coordinate dependence of the dipole moment is given by

$$\text{a) } P_y \sim \operatorname{ch}(\varkappa z)\exp(iq_x x), \quad \text{b) } P_y \sim \operatorname{sh}(\varkappa z)\exp(iq_x x), \quad (2.11)$$

and the dependence of E_y on the coordinates outside the plate is given by (2.9).

To analyze the dispersion equations it is convenient to use an $\omega - q_x$ diagram[13], such as shown in Fig. 1 for the case of simple ionic crystals, when

$$\varepsilon(\omega) = \varepsilon_\infty + \frac{(\varepsilon_0 - \varepsilon_\infty)\omega_{TO}^2}{\omega_{TO}^2 - \omega^2}. \quad (2.12)$$

There are two principal regions on the diagram—radiative R, to the left of the light line, and nonradiative L, to its right. In the region L, the quantity $\varkappa_0$ is real, corresponding in accordance with (2.9) to an exponential decrease of E along the z axis outside the plate. In the region R we have imaginary $\varkappa_0$, and the field outside the plate constitutes an electromagnetic wave propagating away from the plate. It follows therefore that the oscillations whose dispersion curves lie in the nonradiative region of the spectrum are stable, since they are not accompanied by radiation of electromagnetic energy into the surrounding space. In the region R, the oscillations are unstable (virtual[14]) and are accompanied by radiation.

The SO-I in the region L have been investigated in[13]. In this region there exist, in turn, two types of oscillations. The first exist in the region L_2 of Fig. 1, which $\varkappa^2 > 0$. These oscillations are always p-polarized and are described by the dispersion relations (2.7). According to (2.8), they correspond to a dipole moment that decreases away from the surface, so that these modes have a typical surface character. The dispersion dependence for them is shown in Fig. 2.

In crystals in which $\epsilon(\omega)$ is described by formula (2.12), there appear two such modes, the lower of which will be designated ω_- and the upper ω_+. The mode ω_+ corresponds to P_Z oscillations (2.8a) that are symmetrical relative to the center of the plate, and the dispersion relation for this mode is given by (2.7a). The mode ω_- corresponds to antisymmetrical P_Z oscillations (2.8b), and the corresponding dispersion relation is (2.7b). The functions $\omega_\pm(q_x)$ are determined by two dimensionless parameters, $q_x L$ and q_x/q_T, where $q_T = \omega_{TO}/c$ (the third parameter $q_x a \to 0$). If $q_x L \gg 1$ and $q_x/q_T \gg 1$, then the dispersion curves tend to a common limit $\omega_\infty = \omega_{TO}[(\epsilon_0 + \epsilon_M)/(\epsilon_\infty + \epsilon_M)]^{1/2}$, determined from the relation $\epsilon(\omega_\infty) = -\epsilon_M$. At $q_x L \gg 1$, the curves for ω_- and ω_+ merge into a single curve ($\omega_- = \omega_+ \equiv \omega_S$). The dispersion relation for ω_S is given by the relation $\epsilon(\omega_S)\varkappa_0 = -\epsilon_M \varkappa$ or

$$q_x^2 \frac{c^2}{\omega_S^2} = \frac{\varepsilon(\omega_S)\varepsilon_M}{\varepsilon(\omega_S) + \varepsilon_M}. \quad (2.13)$$

We note that in thick crystals, when $q_T L \gg 1$, the inequality $q_x L \gg 1$ is satisfied for all permissible q_x, inasmuch as $q_x \geq q_T$ for the considered modes.

In the case of thin plates ($q_T L \ll 1$) and sufficiently large q_x, the dispersion relations (2.7) take the form

$$\varepsilon(\omega) = -\varepsilon_M \operatorname{th}\left(\frac{q_x L}{2}\right), \quad \varepsilon(\omega) = -\varepsilon_M \operatorname{cth}\left(\frac{q_x L}{2}\right) \quad (2.14)$$

and determine surface modes without allowance for retardation. We note that when the retardation is not taken into account the dispersion curve for ω_- lies be-

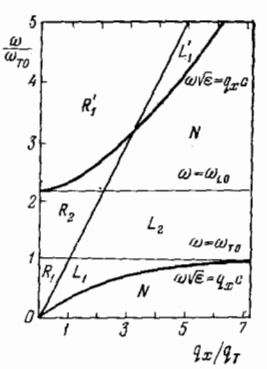

FIG. 1

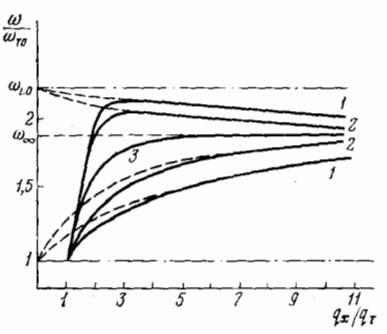

FIG. 2

FIG. 1. $\omega - q_x$ diagram for an ionic-crystal plate. The form (2.12) was used for $\epsilon(\omega)$. The radiative modes are located in the regions R, and the nonradiative ones in the regions L. In the regions N there are no natural oscillations of the plate.

FIG. 2. Dispersion curves for SO-I. Solid curves—with allowance for the retardation, dashed—without retardation. The calculation was made for LiF in vacuum: $\omega_{TO} = 5.78 \times 10^{15}$ sec^{-1}, $\epsilon_0 = 9.27$, $\epsilon_\infty = 1.92$, $\epsilon_M = 1$. Curve 1—$q_T L = 0.1$ ($L \approx 0.57\mu$); 2—$q_T L = 0.2$ ($L \approx 1.14\mu$); 3—$q_T L > 2$ ($L > 11.4\mu$).

tween ω_{TO} and ω_∞, while ω_+ lies between ω_∞ and ω_{LO}. Allowance for the retardation does not change the region of existence of ω_-, but deforms quite strongly the mode ω_+.

For the second type of oscillations in the nonradiative region of the spectrum, $\kappa_0 = -i\eta$ is imaginary. As shown by an elementary analysis of Eqs. (2.7) and (2.10), these modes exist in the regions L_1 and L_1' (see Fig. 1), and they correspond according to (2.8) and (2.11) in the region of the plate to oscillating values of P. According to (2.7) and (2.10), the dispersion relations for these modes take the form

$$\frac{\varepsilon(\omega)}{\varepsilon_M} = \frac{\eta}{\varkappa_0}\operatorname{tg}\left(\frac{\eta L}{2}\right), \quad \frac{\varepsilon(\omega)}{\varepsilon_M} = -\frac{\eta}{\varkappa_0}\operatorname{ctg}\left(\frac{\eta L}{2}\right), \qquad 1 = \frac{\eta}{\varkappa_0}\operatorname{tg}\left(\frac{\eta L}{2}\right), \quad 1 = -\frac{\eta}{\varkappa_0}\operatorname{ctg}\left(\frac{\eta L}{2}\right). \tag{2.15}$$

These are in essence not surface modes, but correspond to an electromagnetic wave propagating inside the plate and "trapped" in it, since its angle of incidence on the boundary between the ionic crystal and the medium exceeds the total internal reflection angle. Numerical calculations of the dispersion relations for these modes are given in[13].

Both types of oscillation modes in the nonradiative parts of the spectrum are characterized by the fact that they do not interact directly with the external electromagnetic wave (with the light), since their dispersion curves lie in a region in which it is impossible to satisfy simultaneously the energy conservation law $\omega = \Omega$ (Ω is the frequency of light) and the momentum conservation law $q_\perp = k_\perp$ (k is the wave vector of the light). Indeed, by combining these two conditions, we have $\omega = (c/\sqrt{\epsilon_M})(k_z^2 + q_\perp^2)^{1/2}$. But since $\omega < cq_\perp/\sqrt{\epsilon_M}$, for nonradiative modes, this condition cannot be satisfied at $k_z^2 > 0$, as can be clearly seen from Fig. 1. The light line on this figure corresponds to the limiting case $k_z = 0$ (the vector k is parallel to the surface of the plate). At all other incidence angles ($k_z \neq 0$) the light curves fall in the region R. Therefore the nonradiative oscillation modes, which lie entirely in the region L, do not intersect the light curves at any value of q_x or k_z. It is possible, however, to produce artificially electromagnetic fields that attenuate along the z axis (in this case $k_z^2 < 0$) and to investigate these modes in optical experiments (see Chap. 6).

In[14] they investigated the roots of the equations (2.7) and (2.10) in the radiative region of the spectrum R, where $\kappa_0 = -i\eta_0$, $\kappa = -i\eta$:

$$-i\frac{\varepsilon(\omega)}{\varepsilon_M} = \frac{\eta}{\eta_0}\operatorname{tg}\left(\frac{\eta L}{2}\right), \quad i\frac{\varepsilon(\omega)}{\varepsilon_M} = \frac{\eta}{\eta_0}\operatorname{ctg}\left(\frac{\eta L}{2}\right), \qquad -i = \frac{\eta}{\eta_0}\operatorname{tg}\left(\frac{\eta L}{2}\right), \quad i = \frac{\eta}{\eta_0}\operatorname{ctg}\left(\frac{\eta L}{2}\right). \tag{2.16}$$

As already noted, these modes are unstable, and the oscillation frequencies obtained by solving (2.16) are complex quantities even if the lattice anharmonicity is not taken into account. The interference of light on passing through a thin plate can be described in terms of these modes. They are in fact volume polaritons perturbed by the surface (see also Chap. 3). A calculation of the coefficients of reflection on absorption of light when light passes through a thin plate under conditions when ϵ depends strongly on ω is given in[27].

b) Sphere[31]. A rather detailed calculation for a sphere is given also in[33], and we confine ourselves here only to a cursory exposition of the results.

The dispersion equation for the electric modes is $P_l = 0$, where

$$P_l = \varepsilon_M [k^i R j_l(k^i R)]' n_l(k^0 R) - \varepsilon(\omega)[k^0 R n_l(k^0 R)]' j_l(k^i R). \tag{2.17}$$

Here $j_l(x)$ and $n_l(x)$ are spherical Bessel and Neumann functions, respectively ($l = 1, 2, \ldots$), and the primes in (2.17) denote differentiation with respect to the argument, while R is the radius of the sphere and $k^i = \omega\sqrt{\epsilon(\omega)}/c$, $k^0 = \omega\sqrt{\epsilon_M}/c$.

The equation for magnetic modes is $S_l = 0$, where

$$S_l = [k^0 R n_l(k^0 R)]' j_l(k^i R) - [k^i R j_l(k^i R)]' n_l(k^0 R). \tag{2.18}$$

The solution for the electric modes (2.17) exist in all three frequency intervals $0 < \omega < \omega_{TO}$, $\omega_{TO} < \omega < \omega_{LO}$ and $\omega > \omega_{LO}$, but at $\omega > \omega_{LO}$ their number is small, and they do not play an important role in that region in the case of interaction with light. At $\omega_{TO} < \omega < \omega_{LO}$ these are SO-I modes, and at $k^i R$, $k^0 R \ll 1$ Eq. (2.17) becomes

$$\varepsilon(\omega) = -\varepsilon_M(l+1)/l. \tag{2.19}$$

The amplitude of the l-th surface mode is proportional to r^{l-1} (r is the distance from the center of the sphere). The frequency ω_1 (at $l = 0$) corresponds to the spherically-symmetrical state[26]. At $\omega < \omega_{TO}$ the solutions of (2.17) constitute a spectrum of volume oscillations deformed by the surface. The magnetic modes (2.18) exist only at $\omega < \omega_{TO}$ and likewise constitute a deformed spectrum of volume polaritons. The oscillation spectrum for a sphere is shown in Fig. 3.

The cross sections for absorption and scattering by a sphere were calculated back in[43] (see also formulas (49)—(60) of[31]). It is shown in[31] that in the harmonic approximation the absorption peaks coincide with the frequencies determined from the equations $P_l(\omega) = 0$ and $S_l(\omega) = 0$, i.e., they coincide with the natural frequencies of the sphere. The same reference contains the numerical calculation of the absorption spectra for spherical NaCl crystals at $R = q_T^{-1} \approx 10\,\mu$ and $R = 0.1$ $q_T^{-1} \approx 1\,\mu$. The results of the calculation for $R = q_T^{-1}$ are shown in Fig. 3. We used in the calculation the expression

$$\varepsilon(\omega) = \varepsilon_\infty + \frac{\varepsilon_0 - \varepsilon_\infty}{1 - (\omega^2/\omega_{TO}^2) - i\gamma(\omega/\omega_{TO})(\omega/\omega_{TO})}, \tag{2.20}$$

where γ is the damping function.

It is thus shown in[31] that the natural oscillations of spherical ionic crystals can be experimentally investigated by infrared spectroscopy methods (see Chap. 5).

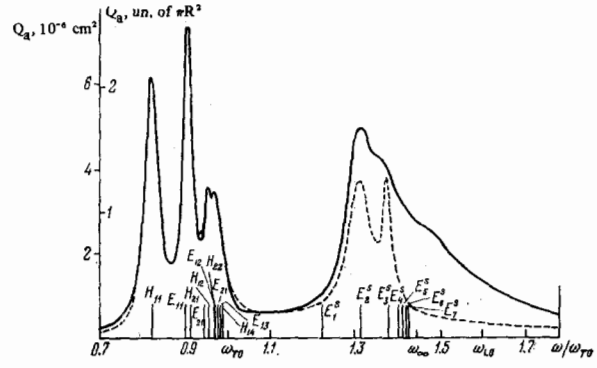

FIG. 3. Frequency dependence of the absorption cross section Q_a for a spherical NaCl crystal in a vacuum at $R = 1/q_T \approx 10\mu$. The dielectric constant is used in the form (2.20): $\omega_{TO} = 3.1 \times 10^{13}$ sec^{-1} (164 cm^{-1}), $\epsilon_0 = 5.934$, $\epsilon_\infty = 2.328$. Solid curves—frequency-dependent $\gamma(\omega/\omega_{TO})$[42], dashed—$\gamma = 0.02$. The vertical lines mark the positions of the natural modes of the oscillations; E—electric modes, H—magnetic modes.

The problem of the SO-I spectrum in a cylinder with allowance for retardation is solved in[32], where the optical spectra are also calculated for scattering of light by a cylindrical ionic crystal. In[30] there is also a calculation of the SO-I spectra without allowance for retardation, for ionic crystals in the form of cylindrical and spherical shells.

The phenomenological calculations have shown that the frequency of optically active oscillations is essentially connected with the crystal configuration. The table indicates the frequency regions in which absorption of light takes place at different crystal configurations. The plus sign stands for the presence of absorption.

A theoretical study of the influence of metallic coatings on the SO-I spectrum was recently initiated[38,173]. It was shown that the presence of a contact with the metal leads, owing to the image forces, to a radical change in the SO-I spectrum at frequencies that are small in comparison with the plasma frequency of the metal.

3. MICROSCOPIC THEORY OF SURFACE OSCILLATIONS

The phenomenological theory of surface oscillations in ionic crystals, which had been successfully developed by 1969, is nevertheless unable to answer a number of fundamental questions:

1) Justify the phenomenological approach and to ascertain the limits of applicability: a) in the limit as $q_\perp a \to 0$ (phenomenology without allowance for spatial dispersion); b) in the region of small $q_\perp$ ($q_\perp a \ll 1$)—phenomenology with allowance for effects of weak spatial dispersion.

2) Find the surface-oscillation spectrum in the entire range of variation of the two-dimensional wave vector $q_\perp$, and not only at $q_\perp a \ll 1$, for macroscopic bodies whose linear dimensions greatly exceed a.

3) Determine the oscillation spectrum of microscopic bodies whose linear dimensions do not greatly exceed the lattice constant a.

4) Find the damping of the surface waves.

A solution of these problems would yield a number of results of importance to the interpretation of experiments in which the surface plays an important role, namely, describe correctly optical experiments and data on electron diffraction, find the thermodynamic functions for samples of small dimensions at arbitrary temperatures, calculate the square of the amplitude (and of the velocity) of the surface-atom oscillations, explain the specific of the Mossbauer effect in finely-dispersed systems, etc.

Answers to these questions can be provided only by a microscopic theory of the lattice vibration in a finite ionic crystal. Problems (1) and (2) have been considered in[16-18,44], and problem (3) in[19,45-52] [3].

Crystal shape	Dimension	$\omega \leqslant \omega_{TO}$	$\omega_{TO} < \omega < \omega_{LO}$	$\omega \geqslant \omega_{LO}$
Cylinder	$q_T R \ll 1$	+	+	
	$q_T R \sim 1$	+	+	
Sphere	$q_T \rho \leqslant 1$	+	+	
Plate:				
normal incidence	$q_T L \leqslant 1$	+		
oblique incidence	$q_T L \leqslant 1$	+		+

a) **Formulation of problem.** In all the references cited here, they considered a plane-parallel plate of an ionic crystal of the NaCl type, and the normal to the surface (the z axis) was directed along the [100] axis. A model of pointlike undeformable ions is used, and it is assumed that the non-Coulomb forces act only between the nearest neighbors (the Kellermann model[1]). Following[3], it is assumed that the presence of a free surface leads only to removal of the interaction forces between the ions located on opposite sides of the surface, but in contrast to[3] this change is not limited to only several atomic planes closest to the surface. It is assumed that the binding forces for the ions on one side of the surface are the same as in an infinite crystal. Cyclic boundary conditions are used in the surface plane of the plate, so that it is possible to introduce a two-dimensional wave vector $q_\perp$, with respect to which the equations of motion are diagonal[16,19]. A solution to the problem of the oscillation of two parallel diatomic chains was obtained in[18] and has made it possible to find the surface oscillations only at $q_\perp = 0$. In general form, the problem of oscillations in an ionic-crystal plate was first formulated in the independently performed studies[16,19], where the equation of motion was expressed in the form

$$\omega^2 M_k u_\alpha \begin{pmatrix} q_\perp, n \\ k \end{pmatrix} = \sum_{\beta, k', n'} D_{\alpha\beta} \begin{pmatrix} q_\perp, n-n' \\ k, k' \end{pmatrix} u_{\alpha\beta} \begin{pmatrix} q_\perp, n' \\ k' \end{pmatrix}; \qquad (3.1)$$

here $u_a \begin{pmatrix} q_\perp, n \\ k \end{pmatrix}$ is the projection on the α axis of the displacement of the ion of type k from the equilibrium position (k = +, − in a diatomic lattice) situated in an atomic layer n = 1, 2, ..., N; M_k is the mass of the ion of type k, and D is the dynamic matrix in the $(q_\perp, n)$ representation.

To find $D \begin{pmatrix} q_\perp, n \\ k, k' \end{pmatrix}$ it is necessary to sum the contributions corresponding to the interactions between the given ion and all the ions located in a certain selected plane. Owing to the presence of Coulomb forces, the corresponding series converges extremely slowly. We recall that in ionic crystals of infinite dimensions there appears in the $(q_\perp, q_z)$ representation a term that is singular at q = 0. This term is eliminated from the equations of motion by introducing a new dynamic variable, the electric field E, which satisfies Maxwell's macroscopic equations[1]. This approach finds its justification in the microscopic theory in Ewald's method, where in the lattice sums are transformed into rapidly converging series. The appearance of a new dynamic variable E in the equations of motion of the lattice leads to a whole number of interesting phenomena: the splitting of the longitudinal ω_{LO} and transverse ω_{TO} frequencies of the optical phonons at q = 0 in accordance with the Lyddane-Sachs-Keller relation, the appearance of piezoelectric properties in crystals without an inversion center[1], a non-analytic dependence of the frequencies of the longitudinal and transverse optical phonons in the region of small q[53,54], etc. The infinite growth of the radius of the inter-ion-interaction as $q \to 0$ has suggested to many workers that the phonon spectrum of an ionic crystal of finite dimensions experiences significant changes in the region $qL \sim 1$[55-59]. It is universally accepted at the present time that the boundaries of the ionic crystal lead not so much to deformation of the volume-oscillation spectrum (although

this effect is quite appreciable in the polariton region), as it does to the appearance of surface phonons of the SO-I type.

It is obvious that in the presence of boundaries the dynamic matrix $D_{\alpha\beta}\binom{q_\perp, n}{k, k'}$ should contain a contribution D^C that decreases slowly at the function of n; this contribution corresponds to the presence of a macroscopic electric field, but now with the boundaries taken into account. To separate this field they used, both in[60] and in[19], the method of θ functions in two-dimensional x, y space (the analog of Ewald's method). It turned out that for $n \neq 0$ we have (see also (23) and (24) of[16])

$$D^C_{\alpha\beta}\binom{q_\perp, n}{k, k'} = -\pi \frac{e_k e_{k'}}{a^2} \frac{\tilde{q}_\alpha \tilde{q}_\beta}{q_\perp} e^{-q_\perp an} \quad (n > 0), \tag{3.2}$$

where e_k is the charge of the ion of type k, and $q_\perp = iq_x + jq_y + kiq_\perp$.

In addition, a contribution D^N, which decreases rapidly over distances of several lattice constants, was separated in[16,19]. This contribution contains the true short-range interaction, renormalized to allow for the Coulomb forces (as in Ewald's method for infinite crystals[1]).

We discuss now the question of the methods used to solve the equations of motion (3.1). For a diatomic crystal it comprises a system of 6N linear homogeneous equations, and the determination of the spectrum reduces to a solution of a determinant of order $6N \times 6N$ (N is the number of atomic layers in the film). Two methods were developed for solving this problem, a numerical one with the aid of a computer[19,45-52] 4) and an analytic one[16,17].

b) Results of numerical calculations for thin films. It is obviously reasonable to use the numerical method of calculating the spectrum from Eq. (3.1) for sufficiently thin films. It is then possible to obtain the dispersion relations $\omega_j(q_\perp)$ $(j = 1, 2, \ldots, 6N)$ for all 6N modes, some of which have a surface character (the amplitude of the oscillations decreases with increasing distance from the surface), and some are of the volume type. The spectrum has been calculated by now for $N = 7$[52] and for $N = 15$[19 45-51].

In[19], the calculation was carried out for NaCl with $q_\perp$ along the [010] axis. Six surface modes of the optical type were observed (Fig. 4), and two surface modes of the acoustic type having the character of Rayleigh waves. No low-frequency surface modes of the SO-I type were observed in that reference[5], and consequently the authors concluded that as $q \to 0$ the phenomenological devices used in[12-14] lead to an incorrect result.

A more detailed investigation of the spectra $\omega_j(q_\perp)$ in the entire two-dimensional Brillouin zone was carried out in[45,46] for $N = 15$ and in[52] for $N = 7$, with additional surface modes of the SO-II type observed in the corners of the zone[45,46]. It was established for the first time in[45] that the SO-I, having an appreciable dispersion with respect to $q_\perp$ (with respect to the parameter $q_\perp L$), cross the volume modes in the long-wave region. Near the crossing points, mode repulsion sets in and mixed surface-volume modes are produced, called quasisurface modes (Fig. 5). Thus, depending on the magnitude and direction of the vector $q_\perp$, the same mode can be both of the surface and of the volume type. In Fig. 5, for example, the mode a at the smallest $q_\perp$ is of the volume type, and then on the section where it

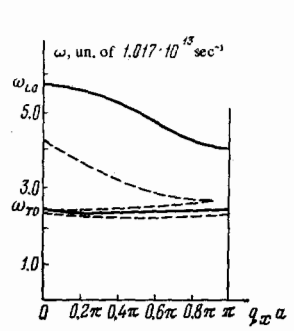

FIG. 4

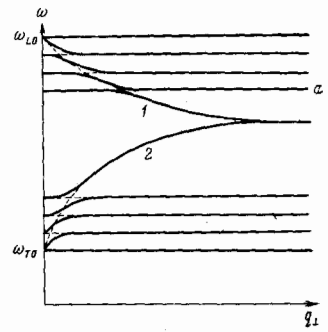

FIG. 5

FIG. 4. Optical volume and surface modes in an NaCl plate 15 atomic layers thick [19]. The dashed lines show the dispersion relations for the surface modes, each of which is doubly degenerate. The dispersion curves of the volume modes lie in the region between the two solid curves.

FIG. 5. Schematic representation of the effect of mode "repulsion" upon intersection of SO-I and volume modes of the oscillations in thin plates of thickness on the order of several lattice constants. 1 and 2—SO-I modes without allowance for retardation. The set of volume modes corresponds to different values of q_z and is discrete in a thin plate. Only the long-wave part of the spectrum ($q_\perp a \ll 1$) is shown. The dashed lines show the surface in volume modes without allowance for their interaction ("repulsion").

coincides with the dashed line it goes over into a surface mode, after which it again becomes a volume mode.

The results of the calculation[52] agree with those of[19] with respect to the number of surface modes and their positions. A thorough analysis of the behavior of the surface modes in the long-wave region has shown, however, that both modes of the SO-I type (the high- and low-frequency modes) are present in the spectrum, but owing to the interaction with the volume modes they become so strongly deformed that the less detailed calculation in[19] is not in a position to identify them correctly[6]. As a result it is concluded in[52] that the phenomenological analysis of SO-I is valid accurate to the interaction with the volume modes. Since the calculations have shown that the influence of this interaction is quite strong, the question of the validity of the phenomenological approach was in fact again raised in[52], inasmuch as this approach does not take into account the interaction of the SO-I with the short-wave volume spectrum (more accurately, with the phonons in the region $q_\perp a \ll 1$, but with arbitrary $q_z a$).

Let us dwell briefly on other numerical calculations of the oscillations of the ion lattice in thin films. In[47] they calculated the square of the amplitude of the ion oscillations in an NaCl film, and in[49] the thermodynamic functions were calculated for the same objects. The frequency spectra for RbF and RbCl films was obtained in[51]. A microscopic analysis of the oscillation modes in an ionic crystal in the form of a rectangular parallelepiped was carried out in[63]. The numerical calculation was carried out for MgO crystals having $4 \times 4 \times 4$ and $6 \times 6 \times 5$ ions along the edges. Since the phenomenological method has not yet yielded the SO-I levels in crystals of this shape, this calculation is of interest, all the more since one measures in the experiment the absorption of light by crystals whose shapes are closer to parallelepipeds than to spheres (in the interpretation of the experimental data for small particles it is customary to use the results of the calculation for a sphere[31]). In[52] they calculated the absorption spectra for light passing through a thin film ($\lesssim 100$ Å) of an ionic crystal. It was shown that a number

of peaks appear in the absorption spectra in the interval between ω_{TO} and ω_{LO}. An approximate method of calculating the absorption spectra for thin films was also developed in[174], based on the use of the dielectric tensor with allowance for spatial dispersion.

Thus, in spite of the obvious accomplishments, the numerical methods have not yielded answers to questions (1), (2), and (4) formulated at the start of this chapter. We note in conclusion that the thicknesses of good films that can be prepared at the present time are such that $N > 10^2$, and the numerical calculations are in this case utterly useless (the resultant determinant is of too high an order). However, the presence of a small parameter $1/N = a/L$ in the problem enables us to find a good analytic solution for thick films (or for a semi-infinite crystal).

c) Analytic method of investigating surface oscillations[16,17]. Were it not for the presence of the contribution D^C (3.2) in (3.1), as is the case in homopolar crystals, then the problem could be solved by the usual procedure[3], in which the problem of finding the surface-oscillation levels is reduced to a system of algebraic equation whose order is equal to the number of atomic planes affected by the surface-perturbation forces. The use of this procedure with the contribution (3.2) taken into account is, however, not very productive, especially at $q_\perp a \ll 1$. A different procedure was therefore proposed in[16], namely a Fourier transformation with respect to n (q_z representation). If we use cyclic boundary conditions along the z axis (i.e., if the two surfaces of the plate are short circuited by each other), then (3.1) becomes diagonalized following the transition to the q_z representation. Instead of the cyclic boundary conditions, one uses here, however, the condition that the surfaces are free, so that (3.1) is not diagonal in q_z. In this representation, however, it is possible to separate in D the contribution corresponding to the dynamic matrix C under the cyclic boundary conditions, which is diagonal in the q_z representation:

$$\omega^2 M_k u_\alpha\left(\begin{matrix}\mathbf{q}\\ k\end{matrix}\right) = \sum_{\beta,\,k'} C_{\alpha\beta}\left(\begin{matrix}\mathbf{q}\\ k,\,k'\end{matrix}\right) u_\beta\left(\begin{matrix}\mathbf{q}\\ k'\end{matrix}\right) + \frac{1}{N}\sum_{\beta,\,k',\,q_z'} \frac{e_k e_{k'}}{\varepsilon^2}\,\Gamma_{\alpha\beta}(\mathbf{q},\mathbf{q}')\,u_\beta\left(\begin{matrix}\mathbf{q}'\\ k'\end{matrix}\right) + \frac{1}{N}\sum_{\beta,\,k',\,q_z'} \Lambda_{\alpha\beta}\left(\begin{matrix}\mathbf{q},\,\mathbf{q}'\\ k,\,k'\end{matrix}\right) u_\beta\left(\begin{matrix}\mathbf{q}'\\ k'\end{matrix}\right), \tag{3.3}$$

where $\mathbf{q} = \{q_\perp, q_z\}$, $\mathbf{q}' = \{q_\perp, q_z'\}$, $q_z = 2\pi n/L$, $n = 1, 2, \ldots, N$. The matrix C coincides with the dynamic matrix of an infinite crystal. In (3.3) are separated two terms that are not diagonal in q_z and describe the influence of the surface. The first, with kernel Γ, is connected with the contribution from the surface long-range forces, and the second, with kernel Λ, is connected with the contribution from the surface short-range forces. Both kernels are sums of products of two functions, one of which depends only on q_z, and the other on q_z':

$$\Gamma_{\alpha\beta}(\mathbf{q},\mathbf{q}') = \exp\left[\,i\frac{a}{2}(q_z' - q_z)\right]\{R_{\alpha\beta}(\mathbf{q}_\perp) f(\mathbf{q}) f(\mathbf{q}') + R^*_{\alpha\beta}(\mathbf{q}_\perp) f^*(\mathbf{q}) f^*(\mathbf{q}')\}; \tag{3.4}$$

$$f(\mathbf{q}) = \left\{2\,\mathrm{sh}\left[\frac{a}{2}(q_\perp + iq_z)\right]\right\}^{-1},$$

$$\Lambda_{\alpha\beta}\left(\begin{matrix}\mathbf{q},\,\mathbf{q}'\\ k,\,k'\end{matrix}\right) = A_{\alpha\beta}\left(\begin{matrix}\mathbf{q}\\ k,\,k'\end{matrix}\right) + A'_{\alpha\beta}\left(\begin{matrix}\mathbf{q}\\ k,\,k'\end{matrix}\right)\exp(iq_z' a). \tag{3.5}$$

The coefficients R, A, and A′ were obtained in[16,17]. The concrete form of Λ (3.5) is connected with the chosen model of the short-range part of the inter-ion forces (interaction between the nearest neighbors only). When the interaction forces with the more remote neighbors are taken into account, terms of the type $A''\left(\begin{matrix}\mathbf{q}\\ k,\,k'\end{matrix}\right)\exp(2iq_z' a)$ etc. appear in the expression for Λ; these terms, however, have the same structure, namely the product of a function of q_z by a function of q_z'.

The equation in the form (3.3) has a number of advantages over (3.1). In the case of thin plates, when N is not too large, the spectrum $\omega_j(q_\perp)$ can be obtained from (3.3) with the aid of a $6N \times 6N$ determinant (q_z takes on N values), similar to what is done with the aid of (3.1). Here, too, however, the calculations are easier than in (3.1), since the matrix C is well known for many crystals, and Γ and Λ are expressed in[16] in terms of simple analytic expressions. At large N, however, when the equation of motion (3.1) is utterly nonproductive, the spectrum can be obtained only from (3.3).

In the limit as $1/N = a/L \to 0$, Eq. (3.3) becomes an integral equation in q_z with a degenerate kernel. Inasmuch as Γ and Λ contain four different products of functions of q_z by functions of q_z', and each product involves six variables (inasmuch as α takes on values and k two values), the total number of obtained homogeneous algebraic equations is 24. It is shown in[17] that the 12 variables stemming from the kernel Γ can be reduced to two, so that the system can be reduced to 14 equations. It is much simpler to obtain a spectrum from a 14-th order determinant, especially at large N, in comparison with (3.1).[7)] It must be particularly emphasized that the principle described above, of reducing the problem of determining the spectrum of the surface waves during an investigation of a 14-th order determinant (in lieu of the initial $6N \times 6N$ determinant) remains valid also for finite N, but the corresponding determinant elements are then expressed in terms of sums (and not integrals) over q_z.

It is convenient to rewrite (3.3) in a somewhat different form[17], which makes it easier to compare it with the equation of motion for an infinite lattice of an ionic crystal. The dynamic matrix C in (3.3) contains contributions from the short-range part of the interaction and from the macroscopic electric field E without allowance for the boundaries. Following[1], we separate from C the contribution due to E, and designate by $\bar{C}$ the remaining part of the matrix, which describes only the short-range interaction in the infinite crystal:

$$\omega^2 M_k u_\alpha\left(\begin{matrix}\mathbf{q}\\ k\end{matrix}\right) = \sum_{\beta,\,k'} \bar{C}_{\alpha\beta}\left(\begin{matrix}\mathbf{q}\\ k,\,k'\end{matrix}\right) u_\beta\left(\begin{matrix}\mathbf{q}\\ k'\end{matrix}\right) - e_k \mathscr{E}_\alpha(\mathbf{q}) + \frac{1}{N}\sum_{\alpha',\,k',\,\beta} \Lambda_{\alpha\beta}\left(\begin{matrix}\mathbf{q},\,\mathbf{q}'\\ k,\,k'\end{matrix}\right) u_\beta\left(\begin{matrix}\mathbf{q}'\\ k'\end{matrix}\right). \tag{3.6}$$

The term $e_k \mathscr{E}_\alpha(\mathbf{q})$ is the sum of the contributions from E and from the term integral in q_z of (3.3), which describes SO-I (with kernel Γ). As shown by analysis[17], $\mathscr{E}$ is the macroscopic electric field with allowance for the crystal boundaries and satisfies Maxwell's equations with the ordinary boundary conditions on the interface between the crystal and the surrounding medium. Allowance for retardation in (3.6) affects only the form of $\mathscr{E}$, which must be determined from the complete system of Maxwell's equations. The term integral in q_z in (3.6) describes the perturbing action exerted by the surface on the short-range forces. Although Eq. (3.6) was derived rigorously in[17] only for the case of a plate, it seems to retain the same form for an arbitrary crystal shape. It is necessary here to use Maxwell's equations for the corresponding surface configuration, and the term that describes the perturbation of

the short-range forces will generally speaking be integral not only in q_z (this is a distinguishing feature of a plate) but in all three projections of q. The equation of motion in homopolar crystals with defects (a surface is a particular case of the defect) takes the form (3.6) if the term $e_k \delta_\alpha(q)$ is omitted.

d) **Results of analytic consideration.** The investigation of Eqs. (3.3) and (3.6) has yielded the following results: In the long-wave part of the spectrum (as $q_\perp a \to 0$ but at arbitrary $q_\perp L$ and $q_\perp c/\omega_{TO}$) the characteristic equation for the surface modes of the SO-I and SO-II type becomes uncoupled, and the 14-th order determinant breaks up into a product of determinants of second and 12-th order. The most determined from the second order determinant are SO-I (they are connected with the presence of an integral term with kernel Γ in (3.3)). On the other hand, the modes obtained from the 12-th order determinant are SO-II (they are connected with the integral term with kernel Λ). As shown in[16], the equations of motion and the dispersion relations for SO-I coincide as $q_\perp a \to 0$ with the phenomenological equations (both without and with allowance for the retardation)[8]. Thus a complete answer to question 1a that must be answered by the microscopic theory is contained in[16].

Reference 16 contains also a calculation of the dispersion of SO-I with respect to $q_\perp a$ at $q_\perp a \sim 1$. It is shown that in the absence of an intersection of the SO-I with the volume modes the dispersion relations for $\omega_\pm(q_\perp)$ can be represented in the form

$$\omega_\pm(q_\perp) = \omega(0) + \Delta\omega_\pm q_\perp a. \tag{3.7}$$

The quantity $\Delta\omega_\pm$, in particular, depends on the interaction between SO-I and SO-II, i.e., on the model of the surface. Since the SO-II amplitude decreases at distances on the order of a, the behavior of SO-II depends on the microstructure of the real surface of the crystal. In the real situation, therefore, the position of the SO-II levels has a statistical scatter, forming a two-dimensional phonon spectrum similar to the spectrum of a disordered system. For the same reason, the dispersion curves for SO-I also have a certain statistical scatter, the width of which tends to zero as $q_\perp a \to 0$. At $q_\perp a \sim 1$, the principal difference between SO-I and SO-II disappears, for in this case the SO-I amplitude decreases away from the surface at distances $1/q_\perp \sim a$.

It was noted earlier that a numerical calculation with the aid of (3.1) has shown that a mode repulsion effect takes place at the intersection of SO-I with the volume spectrum. With increasing plate thickness, the density of the volume modes increases, and the spectrum of the volume oscillations becomes continuous. Increasing hypothetically the volume-mode density in Fig. 5, we note that the surface mode constitutes in this case a trail made up of infinitesimally small influctions of the volume-oscillation modes. The ω-q_x diagram of Fig. 6 shows the intersection of SO-I with the continuous one-dimensional volume spectrum corresponding to different values of q_z in the entire Brillouin zone (the dispersion of the volume modes with respect to $q_\perp a$ can be disregarded, since the SO-I exist in the region $q_\perp a \ll 1$). Since the numerical calculations in[45,52] do not make it possible to identify the parameter with which the mode-repulsion effect is connected, an analytic calculation of the quasisurface modes was carried out in[17]. It was shown that the corresponding directions are small in terms of the parameter $q_\perp a$. In other

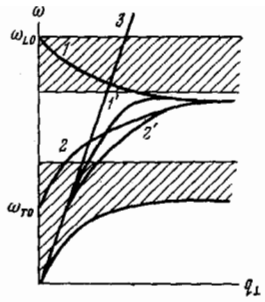

FIG. 6. Intersection of SO-I with the continuous spectrum of the volume oscillations in the long-wave region $q_\perp a \ll 1$. 1, 2) surface modes without allowance for retardation, 1', 2') the same modes with allowance for retardation. The shaded regions are occupied by the continuous spectrum corresponding to the volume-oscillation frequencies at q_z ranging from $-\pi/a$ to π/a and at $q_\perp = 0$; 3) optical branch $\omega = cq_\perp$. The lower limit of the transverse volume oscillations is drawn with allowance for retardation and corresponds to the equation $\omega^2\epsilon(\omega) = c^2q_\perp^2$.

words this interaction can be disregarded in the limit as $q_\perp a \to 0$ (corresponding to the phenomenological approach without allowance for the spatial dispersion). Taking into account the corrections small in $q_\perp a$, the equation for the SO-I frequencies in the presence of intersection takes the form[17] (cf. (2.7)):

$$\begin{aligned}
&\frac{\varkappa_\perp}{\varepsilon Q_\perp}\operatorname{cth}\left(\frac{\varkappa_\perp L}{2}\right)+1 = \\
&= -\frac{q_\perp}{Q_\perp}\frac{aq_\perp}{4\pi}\int_{-\pi/a}^{\pi/a} d(aq_z)\left[\left(\frac{aq_z}{2}\right)^{-2}\frac{1}{\varepsilon}\right. \\
&\qquad \left. -\sin^{-2}\left(\frac{aq_z}{2}\right)\frac{1}{\varepsilon_{\parallel}(q_z)}\right], \\
&\frac{\varepsilon Q_\perp}{\varkappa_\perp}\operatorname{cth}\left(\frac{\varkappa_\perp L}{2}\right)+1 = \\
&= \frac{aQ_\perp}{4\pi}\int_{-\pi/a}^{\pi/a} d(aq_z)\left[\left(\frac{aq_z}{2}\right)^{-2}\varepsilon\right. \\
&\qquad \left. -\sin^{-2}\left(\frac{aq_z}{2}\right)\varepsilon_\perp(q_z)\right];
\end{aligned} \tag{3.8}$$

Here $\epsilon_\parallel \equiv \epsilon_{zz}$, $\epsilon_\perp \equiv \epsilon_{xx}$ are the components of the dielectric tensor with allowance for the spatial dispersion (at $q_\perp = 0$). Thus, to obtain corrections that are small in $q_\perp a$ to the dispersion law obtained on the basis of the phenomenological approach without allowance for the spatial dispersion it is necessary to know the function $\epsilon(\omega, q_z)$ in the entire Brillouin zone (but at small $q_\perp a$), i.e., these corrections cannot be obtained by taking into account only the corrections to $\epsilon(\omega)$ that are small in qa. We note also that the factor $\sin^{-2}(aq_z/2)$ in (3.8) cannot be obtained in the continual approximation, since it is entirely due to the periodicity of the lattice. All the foregoing, however, must not be taken to mean that attempts at any phenomenological description of SO-I with allowance for spatial dispersion are unreasonable. The right-hand side of (3.8) is nevertheless expressed in terms of $\epsilon(q_z, \omega)$ (although at arbitrary $q_z a$), and the appearance of the factor $\sin^{-2}(aq_z/2)$ can be easily understood and can be readily accounted for by modifying our analysis to take the discreteness of space into account[17].

The main positive result of the investigation of (3.8) was the observation of a broadening of the SO-I levels due to intersection with the continuous volume spectrum. This result becomes understandable if it is recognized that the quasisurface oscillation goes over into a volume oscillation without absorption or emission of energy quanta. A similar situation, as is well known (see, e.g.[64]) arises also for quasilocal oscillations. The harmonic broadening is determined almost completely

by the density of the one-dimensional (i.e., $q_\perp = 0$, $q_z \neq 0$) volume spectrum $\omega_j(q_z)$ at the point of intersection with SO-I. Near the van-Hove singularity, where $d\omega_j(q_z)/dq_z = 0$, the density of states is maximal (in the one-dimensional spectrum the density of states at this point has a root singularity), and the line width is of the order of $\omega_{TO}(q_\perp a)^{2/3}$. For wavelengths on the order of optical this broadening is $\sim(10^{-2} - 10^{-3})\omega_{TO}$, i.e., it becomes comparable with the anharmonic broadening and can be observed in experiment. Far from the van Hove singularities this broadening is $\sim\omega_{TO}q_\perp a \sim 10^{-4}\omega_{TO}$ and becomes very weak. This situation recalls the broadening of the energy levels of a bound electron-phonon state in a quantizing magnetic field near their intersection point[85]. It is also shown in[17] that the virtual modes that appear in the phenomenological approach[14] can be interpreted as a result of the intersection of the SO-I with volume polaritons.

A recent paper[175] is also devoted to the dispersion of the SO-I modes with respect to the parameter $q_\perp a$ at $q_\perp a \ll 1$, and also to their broadening as a result of the intersection with the volume-oscillation spectrum. In[175] they actually used a phenomenological method of calculation, Maxwell's equations with allowance for weak spatial dispersion in the expression for the dielectric tensor. Neglect of the role of SO-II and allowance for only the weak spatial dispersion has led in[175] to results that differed somewhat from[16,17]. First, no splitting of the SO-I modes as a result of the dispersion with respect to $q_\perp a$ was found (according to[175], $\Delta\omega_+ = \Delta\omega_-$ in formula (3.7)). No increase was observed in the broadening of the SO-I levels near the van Hove singularities (if only weak spatial dispersion is taken into account, the frequency of the volume phonons varies like q^2 and there are no van Hove singularities in the spectrum). It should be noted that there is no universally accepted procedure at present for taking the boundaries into account within the framework of crystal optics with allowance for weak spatial dispersion, and this question is under lively discussion in the literature (see, e.g.,[176]).

We note in conclusion that in spite of the considerable progress in the construction of the macroscopic theory of surface oscillations in ionic crystals, question (4) formulated at the start of this chapter has not been investigated at all to date. It is necessary to take the SO-I damping into account in phenomenological calculations of light absorption by crystals of finite dimensions. Anharmonic effects are usually taken into account by introducing an imaginary part of $\epsilon(\omega)$ (see e.g., (2.20)), and the anharmonic constants are assumed equal to the corresponding values for massive crystals. However, the use of ϵ of the massive sample is justified in the macroscopic theory only in the harmonic approximation. In some cases, the experimental line width turns out to be larger than the calculated one.

Since anharmonic effects are generally speaking due to the interaction of the SO-I with volume phonons of any wavelength (including short-wave phonons), the mechanical use of complex ϵ of a massive sample in the calculations is hardly justified for crystals with finite dimensions. The microscopic theory is therefore faced at present with the very pressing problem of finding the SO-I level width due to lattice anharmonicity.

4. INTERACTION OF ELECTRONS WITH SURFACE PHONONS

The study of the interaction of electrons with surface optical phonons is of interest for two reasons.

First, surface phonons can be observed in experiments on electron-beam diffraction[20,66,67].

Second, the interaction with surface phonons should influence the kinetic coefficients in small-size samples and in thin films. By way of example of such an experimental situation, we can mention, for example, magnetophonon resonance in semiconducting films or the influence of surface oscillations on the high-frequency electric conductivity of finely-dispersed systems based on polaron superconductors[179].

The diffraction of fast electrons can be calculated with the aid of standard phenomenological procedures using the equations of electrodynamics. The first such calculations (without allowance for retardation) was carried out for the losses of fast electrons passing through a thin metal plate[8] (see also[68]). The results for surface plasmons can be easily generalized to include the case of surface phonons, by representing $\epsilon(\omega)$ in the form (2.24). According to[8], the probability that an electron with momentum $\hbar k_\perp$ in the plane of the plate loses an energy $\hbar\omega$ is

$$P(\mathbf{k}_\perp, \omega) = P_V(\mathbf{k}_\perp, \omega) + P_S(\mathbf{k}_\perp, \omega), \tag{4.1}$$

where

$$P_S(\mathbf{k}_\perp, \omega) = -\frac{e^2}{\pi^2\hbar v^2}\frac{k_\perp}{[k_\perp^2 + (\omega/v)^2]^2}\operatorname{Im}\left\{\frac{1-\varepsilon(\omega)}{\varepsilon(\omega)}\times\right. \\ \left.\times\frac{2[\varepsilon(\omega)-1]\cos(\omega L/v) + [1-\varepsilon^2(\omega)]\exp(k_\perp L) - [1-\varepsilon(\omega)]^2\exp(-k_\perp L)}{[1-\varepsilon(\omega)]^2\exp(-k_\perp L) - [1+\varepsilon(\omega)]^2\exp(k_\perp L)}\right\}, \tag{4.2}$$

$$P_V(\mathbf{k}_\perp, \omega) = -\frac{e^2}{2\pi^2\hbar v^2}\frac{L}{k_\perp^2 + (\omega/v)^2}\operatorname{Im}\frac{1}{\varepsilon(\omega)}; \tag{4.3}$$

Here v and e are the velocity and charge of the electron and L is the thickness of the plate. The loss functions P_V and P_S are connected with the interaction of the electron with the volume and surface phonons, respectively. $P_S(k_\perp\omega)$ contains poles that coincide with the positions of the surface-phonon frequencies ω_+ and ω_-, which are defined by formulas (2.14) (see also Fig. 2). In experiment one usually determines the integrated loss function

$$P(\omega) = 2\pi\int_0^K dk_\perp k_\perp P(\mathbf{k}_\perp, \omega), \tag{4.4}$$

where $\hbar k = \theta(2mE)^{1/2}$ is the uncertainty of the momentum (θ is the electron scattering angle relative to the primary axis, and m and E are the electron mass and energy). In the calculations it is also taken into account that one measures in the experiment a characteristic that is integrated not only with respect to $k_\perp$ but with respect to ω:

$$\bar{P}(\omega) = \frac{1}{2\Delta}\int_{\omega-\Delta}^{\omega+\Delta} d\omega' P(\omega'). \tag{4.5}$$

Expressions (4.1) and (4.2) were numerically integrated in[68] (see also[69]) with respect to $k_\perp$ and ω for the parameters of LiF ($\epsilon_\infty = 1.92$, $\epsilon_0 = 9.27$, $\omega_{TO} = 5.78\times10^{13}\ \text{sec}^{-1}$, $\gamma = 0.045$) and the experimental conditions prevailing in the study of the passage of fast electrons through an LiF plate[20], namely E = 25 keV, $\theta = 10^{-4}$ rad, and $\hbar\Delta = 0.01$ eV. The experimental and calculated relations for the loss function are shown in Fig. 7. The frequency averaging of (4.5) over the inter-

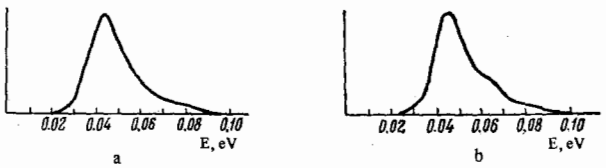

FIG. 7. Experimental (a) [20] and theoretical (b) [66] spectra of the energy losses E of fast electrons (25 keV) on passing through an LiF plate 240Å thick.

val 2Δ ($\hbar\Delta$ is the accuracy with which the energy is determined when the losses are measured) leads to a complete "smearing" of a narrow beam at a volume-phonon frequency $\omega = \omega_{LO}$.

In[70,71] the integration with respect to $k_\perp$ in (4.4) was carried out analytically for the case of weak damping ($\gamma \to 0$), and in[71] account was taken of the additional pole of the function $P_S(k_\perp, \omega)$ at $\epsilon = 0$, i.e., at the frequency $\omega = \omega_{LO}$. The presence of this pole in PS decreases the amplitude of the peak connected with the interaction of the electron with the volume polarization oscillations at $\omega = \omega_{LO}$. This phenomenon is called in the literature the limitation (Begrenzung) effect[20].

In[70] they also calculated the losses of the fast electrons with allowance for retardation. It was shown that in this case a peak appears in the frequency region $\omega \lesssim \omega_{TO}$, due to Cerenkov radiation. However, the amplitude of the Cerenkov peak is lower by three orders of magnitude than the peak at $\omega = \omega_{LO}$.

The classical method used in[8] to calculate the loss in a beam of fast electrons, cannot be employed for a theoretical investigation of many physical situations, such as the calculation of kinetic coefficients with allowance for the interaction of the electron with the SO-I, of the electron scattering cross sections with allowance for multiphonon processes, etc. It is most convenient to formulate such problems from the very outset in the quantum-mechanical approach, and to this end it is necessary to determine the quantum-mechanical expression for the Hamiltonian of the interaction between the electron and the SO-I.

In[71-73] a quantum-mechanical expression was obtained independently for the Hamiltonian of the interaction between an electron and lattice vibrations in an ionic-crystal plate. It was shown that this Hamiltonian (which we shall designate H_{int}) receives contributions from both volume and surface modes of the SO-I type. A canonical transformation that makes it possible to decouple completely the contributions from the surface and volume modes, by representing them in additive form, has been obtained in[73].

The form of H_{int} (see formulas (3.4) of[71] and (36)–(38) of[73]) is quite similar to the Fröhlich Hamiltonian for the electron-phonon interaction in an infinite crystal[74] [9]. The constants for the electron-phonon interaction in the plate (including also the constants for the electron interaction with the SO-I) and in an infinite crystal are of the same order of magnitude (see formula (39) of[73]).

It was noted in[71-73] that in the region outside the plate the SO-I produce an electric field that decreases slowly away from the surface, and consequently an electron located outside the plate interacts with the surface phonon oscillations. The volume modes produce no field oscillations in the space outside the plate, so that these modes interact only with the electrons inside the plate.

It was noted in[73] that the field produced by the volume oscillations orthogonalized to the surface oscillations is not a purely periodic function of the coordinate z (as is always the case in the spatially-homogeneous case of an infinite crystal), but has a contribution that decreases away from the surface; this contribution is responsible for the limiting effect that appears in the electronic-loss spectra at the frequency $\omega = \omega_{LO}$.

The diffraction of slow electrons reflected from the surface of a crystal was calculated in[75] (for plasmons) and[76] (for phonons) with the aid of the Hamiltonian for the interaction of an electron with SO-I. This is accompanied by absorption or emission of surface phonons as a result of the interaction of the SO-I field with the electron outside the crystal. As noted above, the fields produce no volume oscillations in this region, so that the diffraction spectra have no singularities in the case of reflection of a beam of slow electrons from the surface of the crystal at the frequency of the volume polarization oscillations $\omega = \omega_{LO}$.

The energy spectrum of slow electrons (1–100 eV) following reflection from a flat surface of single-crystal ZnO was measured in[67]. The experimental curves (Fig. 8) show peaks of no-phonon reflection, of reflection with emission of 1, 2, and 3 phonons, and a peak with absorption of one phonon; the latter, as expected, decreases rapidly with decreasing temperature. The measured frequencies of the one-phonon peaks turned out to be 68.8 MeV and 67.6 meV for reflection from the faces $(1\bar{1}00)$ and (0001), respectively, i.e., a weak anisotropy was observed. These frequencies coincide, within the limits of the measurement accuracy, with those calculated from the condition $\epsilon_\perp(\omega) = -1$, where $\epsilon_\perp$ is the dielectric-tensor component normal to the surface[10].

The experimental results obtained in[67] were compared in[76] with the results of calculation for single-phonon processes. The experimental and calculated data for the corresponding peak are in good agreement.

The question of quantum-mechanical calculation of the scattering cross section in the collision between an electron and a surface phonon was raised in recent papers[77,78] [11]. Inasmuch as in the calculations of[71,75,76] the electron is assumed to be a classical par-

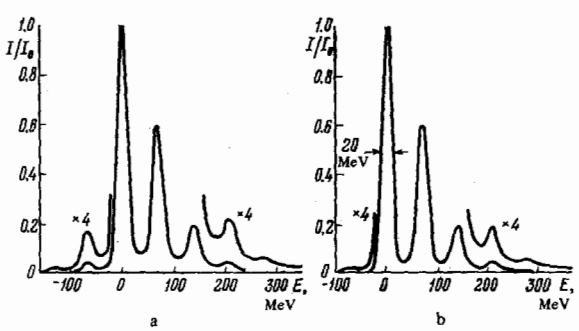

FIG. 8. Spectrum of energy losses E of the slow electrons (7.5 eV) upon reflection from the surface of single-crystal ZnO [67] at temperatures 286°K (a) and 127°K (b). I and I_0 are the intensities of the reflected and incident electron fluxes, respectively.

ticle, the authors of[78] hope that their approach is more consistent when it comes to calculating electron diffraction. Incidentally, the results obtained in[78] for the single-phonon scattering cross section practically coincide with[76]. The same agreement with[76] was observed also for multiphonon processes, a quantum mechanical calculation of which is given in[80]. In[177] there is also a calculation of the diffraction of slow electrons with allowance for their penetration into the interior of the crystal.

A study of bound states of an electron in a crystal with surface phonons was recently initiated with the aid of a Hamiltonian obtained for the interaction between the electron and the surface phonons. A theoretical investigation of the large-radius surface polaron, with allowance for SO-I, is carried out in[81,178]. The absorption of light due to small-radius surface polarons was calculated in[179] and the results have shown that the absorption peak for small-radius surface polarons is shifted towards shorter wavelength relative to volume polarons. It is reported in[179] that this effect was observed experimentally in small TiO_2 crystals.

5. SPECTROSCOPIC INVESTIGATIONS OF SURFACE OSCILLATIONS IN SMALL CRYSTALS

It appears that the first manifestation of surface oscillations were distinctly observed in the infrared spectra of small crystals. The object of the investigation in this case is, of course, a conglomerate of such crystals, placed on some substrate or pressed into a matrix made of a material that is transparent in the given region of the spectrum. The standard procedure used in infrared spectroscopy for the investigation of powders employs precisely such objects (KBr tablets pressed in polyethylene, suspensions in mineral oil, etc). This method is widely used in particular, to determine the oscillation frequencies in those cases when the production of sufficiently large single crystals is difficult. Many investigators have noted long ago that the lattice-oscillation frequencies obtained by this method do not have good reproducibility, depend on the crystal dimensions and on the method of pellet preparations, etc. These "anomalies", as shown by a comparison[32] of the oscillation frequencies obtained for powders and single crystals of various substances, are due to a considerable degree, if not entirely, to the surface (size) effect. It appears that this effect was first used in[82] to explain the observed discrepancy between the frequencies obtained from the powder spectrum and the reflection spectrum of UO_2 single crystals.

As already indicated, surface polaritons in crystals in which at least two dimensions are small in comparison with $(\omega_{TO}/c)^{-1}$ (sphere, thin cylinder) are radiating and should therefore become manifest in the absorption spectra. Calculations performed in[31] for the cross section for light absorption by spherical particles at $\omega_{TO}R/c = 1$ and 0.1 ($R = 10$ and 1 μ respectively for NaCl) show that in this interval one should expect a noticeable decrease of absorption at the volume modes ($\omega \lesssim \omega_{TO}$) and simultaneous appearance of absorption on the surface modes in the region $\omega_{TO} < \omega < \omega_{LO}$. According to (2.19), in the limiting case of minute crystals of spherical shape ($\omega_{TO}R/c \ll 1$), the position of the first ("Frohlich") mode ($l = 1$) is determined from the condition $\epsilon(\omega_1) = -2\epsilon_M$, i.e.,

$$\omega_1^2 = \omega_{TO}^2 \frac{\varepsilon_0 + 2\varepsilon_M}{\varepsilon_\infty + 2\varepsilon_M}. \qquad (5.1)$$

Inclusion of the anharmonicity leads to the appearance in the absorption spectrum of a band with a position corresponding to

$$\varepsilon'(\omega) \equiv \mathrm{Re}\,\varepsilon(\omega) \approx -2\varepsilon_M. \qquad (5.2)$$

The absorption due to modes of higher order ($l = 2, 3, \ldots$) can be neglected in this case, although at larger particle dimensions this is not generally the case.

For a quantitative calculation of the absorption spectrum it is necessary to know the optical constants of the investigated crystals, i.e., $\epsilon'(\omega)$ and $\epsilon''(\omega)$, in a wide frequency interval, it is also useful to make a more detailed comparison with theory for simple cubic crystals with one dispersion oscillator. This is the reason why many such investigations were performed with alkali-halide crystals and also with MgO.

The situation is more complicated with the crystallite shape, which usually differs from the spherical shape assumed in the calculation. Crystals obtained by evaporation of a saturated aqueous solution[21,83] have usually the shape of cubes or parallelepipeds and those obtained by pulverizing larger crystals have irregular shapes. First of all, it is difficult to estimate the error due to this circumstance. One can hope that in the limiting case of very small crystals (in all three dimensions) their shape does not play an important role. A comparison of spectra obtained in[84] for cubic and spherical KBr particles seems to favor this hypothesis, as do also results obtained in[85] for NaCl particles with dimensions ~70 Å, introduced into porous glass.

There are many experimental investigations of the absorption spectra of minute alkali-halide crystals[21,86-87]. In[21,86], minima were observed in the transmission spectrum between ω_{TO} and ω_{LO} (see Fig. 9) of KCl and NaCl crystals with dimensions 5–10 μ, pressed into polyethylene. In[87], the spectrum shown in Fig. 9 was compared with calculation for spherical particles, assuming R to be 8 μ. The discrepancy between the positions of the calculated and experimental peaks amounted in this case to about 10 cm^{-1}.

An investigation of the infrared spectra of NaCl and KBr particles, with linear dimensions d from 40 to 2 μ, pressed into paraffin, was undertaken in[83]. This range of dimensions includes both the case $\omega_{TO}d/c < 1$ and the transition region $\omega_{TO}d/c \sim 1$, where a "spill-over" of the absorption intensity from the volume to the surface modes could be expected. Analogous measurements for KBr crystals in polyethylene were carried out in[84]. Fig. 10 shows the corresponding spectra for NaCl. For the largest crystals (curve 1), the spectrum was characterized by two broad bands of approximately equal intensity: low-frequency, adjacent to ω_{TO} on the long-wave side, and a band between ω_{TO} and ω_{LO} (approximately 175 cm^{-1}). The decrease in the crystal dimensions leads to a relative attenuation of the low-

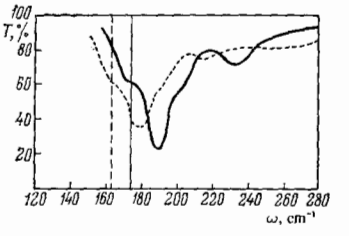

FIG. 9. Transmission spectrum of minute NaCl crystals pressed into polyethylene at 7°K (solid curve) and 290°K (dashed) [86]. The vertical lines mark the positions of ω_{TO} at these temperatures (175 and 164 cm^{-1}, respectively).

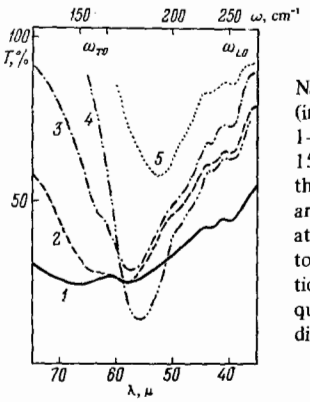

FIG. 10. Transmission spectra of NaCl crystals of different dimensions d (in microns) pressed in paraffin [83]: 1–d = 20–40, 2–d = 10–20, 3–d = 7–15, 4–d < 3, 5–d < 2. The positions of the limiting frequencies ω_{TO} and ω_{LO} are indicated. The secondary structure at 235 and 254 cm^{-1} is apparently due to two-phonon processes with participation of short-wave phonons, whose frequencies do not depend on the crystal dimensions.

frequency band, and subsequently to a complete vanishing[12] at $d \lesssim 3\ \mu$. The position of the high-frequency band shifts in this case towards higher frequencies, and reaches 191 cm^{-1} at $d \sim 2\ \mu$. Similar results were obtained also for KBr both in[83] and in[84]. The limiting value at $d \sim 3$ was 126 cm^{-1} according to[83]. In [84] is given a somewhat higher frequency—130 cm^{-1} ($d = 9$ ($d = 0.3\ \mu$). A quantitative comparison with the theory was carried out in[83] for particles that were "monochromatized" with respect to the dimensions, $d = 10 \pm 2\ \mu$. The position of the peak in the absorption spectrum (184 cm^{-1}) turned out to be somewhat lower than the calculated value for spherical particles of the same diameter (190 cm^{-1}). The expression for the dielectric constant used in these calculations was of the form (2.20) with a frequency-dependent damping function $\gamma(\omega)$ determined in[42]. The limiting value for small NaCl particles (191 cm^{-1}) is compared in[83] with the position of the Frohlich frequency (203 cm^{-1} at $\epsilon_M = 2$). This discrepancy practically vanishes if the position of the peak is determined from (5.2) and account is taken not only of the damping but also of the anharmonic shift $\Delta(\omega)$, introducing it into the expression for $\epsilon(\omega)$ (see, e.g.,[88]):

$$\varepsilon(\omega) = \varepsilon_\infty + \frac{(\varepsilon_0 - \varepsilon_\infty)\,\omega_0^2}{\omega_0^2 + 2\omega_0\Delta(\omega) - \omega^2 + i\omega_0\Gamma(\omega)}, \qquad (5.3)$$

where $\Gamma(\omega) = \gamma(\omega)\omega$, and ω_0 has the meaning of the harmonic TO frequency. A similar procedure for taking anharmonicity into account was carried out recently in[89] using the functions $\Delta(\omega)$ and $\Gamma(\omega)$ determined from reflection experiments.

However, the experimentally obtained widths of the bands exceed noticeably (by 2–3 times) the calculated values. We shall discuss this circumstance later on. We note here only that so strong a broadening seems to prevent observation of the theoretically-predicted fine structure of the spectrum.

The application of the theoretical concepts developed above to conglomerates of minute crystals calls for the preparation of research samples with sufficiently small particle concentrations, so that the distance between particles exceeds the wavelength of the light. A noticeable influence of particle interaction on the optical spectra was observed in[83,90,180]. An increase in the particle concentration shifts the absorption band towards lower frequencies.

In[90,91] they investigated samples made up of minute MgO crystals. The use of the functions $\epsilon'(\omega)$ and $\epsilon''(\omega)$ from[92] has made it possible in[90] to obtain satisfactory agreement between the positions of the calculated peaks and the experimental ones. To explain the widths of the peaks, however, it was necessary to assume that Γ is eight times larger than the corresponding volume quantity. A similar result was obtained for NiO in[181].

Absorption by NaCl particles with dimensions of several dozen Angstroms was investigated in[85]. When the transparency is measured for such small crystals it is certainly possible to neglect the scattering of light in comparison with the "true" absorption. The result obtained in[85] namely the agreement between the absorption band and the value calculated from the phenomenological theory, is in itself not trivial for such small particles. Let us dwell briefly on results obtained with anisotropic crystals. One of the first studies[23] in which the discussed effect in infrared spectra was investigated at all was carried out on minute AlN crystals with wurtzite lattice. Figure 11, which is taken from[23], illustrates clearly the dependence of the surface-mode frequencies on the matrix dielectric constant ϵ_M, which ranged in[23] from 1 to 4. The investigated mixture consisted of both long needle-like crystallites and of crystals of cubic shape. This together with the presence of two IR active frequencies was the reason for the appearance of three surface modes in the spectrum.

The limiting case of minute TiO_2, SnO_2, and $BaTiO_3$ crystals was investigated in[22,93]. In the presence of several (n) dispersion oscillators we have in place of (5.1)

$$\prod_{i=1}^{n}\left(\frac{\omega_{Li}}{\omega_{TOi}}\right)^2 = \frac{\varepsilon_0 + 2\varepsilon_M}{\varepsilon_\infty + 2\varepsilon_M}. \qquad (5.4)$$

The positions of the peaks in the calculated and experimental spectra are close, but the widths of the peaks in experiment are again much larger. For the left- and right-hand sides of (5.4) the values obtained for SnO_2 were 1.40 and 1.47. The agreement is somewhat worse for TiO_2, viz., 2.45 and 2.98.

We note also a number of investigations of the infrared spectra of minute crystals. The appearance of surface oscillations in the thermal-radiation spectra of a number of crystals was observed in[94]. Calculations in which the scatter of the dimensions of spherical or cylindrical particles is taken into account are compared with experiment in[95,180]. The influence of the formally introduced additional damping (in comparison with the volume damping) on the form of a spectra and

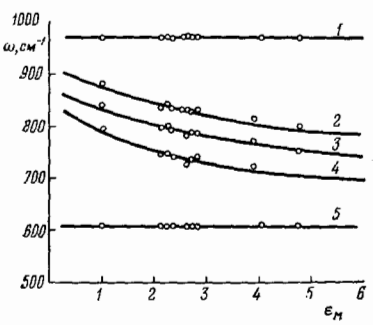

FIG. 11. Positions of the minima in the transmission spectrum of minute AlN crystallites vs. the dielectric constant of the medium [23]. The frequencies corresponding to curves 1 and 5 (965 and 610 cm^{-1}) correspond to a volume mode and do not depend on ϵ_M. Curves 2–4 correspond to surface modes.

on the widths of the bands is illustrated by the results of numerical calculations in[182]. The influence of the crystallite dimensions on the position of the lines in Raman-scattering spectra was noted and discussed in[96-98,183].

Summarizing, we can state that the qualitative picture of the optical properties of minute crystals agrees with the predictions of the theory. In a number of cases, there is also good quantitative agreement. The quantitative comparison of theory and experiment becomes in itself possible only if the form of the function $\epsilon(\omega)$ is sufficiently well known, since the positions of the bands in the spectra are quite sensitive to variation of the real part of this function. A more complicated question is that of the nature of the observed additional broadening of the bands. It is still not clear whether the latter is connected to some degree with the anharmonic interaction of the surface and volume modes or is due to the large number of defects in the crystals investigated so far. Some light could be cast on this question by measurements in a wide range of temperatures using particles that are carefully "monochromatized" with respect to dimensions. An additional source of broadening for particles of cubic or near-cubic shape may be the appearance of several surface modes of close frequency even at crystallite dimensions that are extremely small in comparison with the wavelength[184]. These frequencies, not being resolved, can produce in experiment a single broadened spectral distribution.

Finally, a last remark. It must be borne in mind that the determination of lattice-vibration frequencies in ionic crystals from spectra obtained with powders should be approached with great caution[13]. For binary crystals one can use in first-order approximation the Fröhlich formula (5.1) in the region where it is valid (i.e., at $d \ll \lambda$), working with strongly diluted compositions.

6. OPTICAL INVESTIGATIONS OF SURFACE OSCILLATIONS IN "SEMI-INFINITE" CRYSTALS AND IN THIN FILMS

As already mentioned in Chap. 4, surface oscillations in plates and in films of ionic crystals were observed experimentally in the analysis of the energy-loss spectra following electron scattering. However, the resolution of the electron-spectroscopy methods is lower by approximately two orders of magnitude than the resolution of standard grating spectrometers for the far infrared region. Thus, for example, in[67] the resolution was approximately 160 cm^{-1}, practically equal to the entire dispersion width of the surface phonons in the investigated crystal. At the present time this limits strongly the capabilities of the procedure when it comes to measuring phonon damping, to plotting the dispersion curves, etc. Naturally, it seemed attractive to perform the corresponding investigations by infrared-spectroscopy methods. The interpretation of such experiments in plate geometry would be free of a number of factors that complicate it in the case of minute crystals (the shape factor, interaction between particles) and would yield a noticeably large volume of information.

However, unlike the case of minute crystals, surface modes in a plate are nonradiative, i.e., they do not interact with light in experiments on absorption and reflection (this, of course, does not include the possibility, in principle, of manifestation of surface phonons in Raman-scattering spectra[37,100]). The absence of interaction with light is due to the fact that, as already noted above (Chap. 2), $\omega < cq_x$ over the entire dispersion curve (the phase velocity of the surface waves is lower than the velocity of light and the dispersion curves $\omega(q_x)$ do not cross the light line $\omega = ck_x$) (Fig. 12).

It was shown in Chap. 2 that the energy and momentum conservation laws in the interaction of surface phonons with light, on the one hand, and the form of the dispersion curves on the other, do not contradict each other only if the electromagnetic wave attenuates along the z axis in the space surrounding the investigated plate. Such an inhomogeneous wave propagating along the interface in the plane of incidence and attenuating exponentially in the direction of the optically less dense medium is produced in the case of total internal reflection. This wave is not transverse, since the component of E in the propagation direction differs from zero (see, e.g.,[101]). A few years ago, a modified method of perturbed total internal reflection (PTIR) was proposed[102a] for the investigation of surface plasmons in metals.[14] It was recently used also for the investigation of surface phonons[24]. The geometry of the experiment and the employed notation are explained in Fig. 13. An electromagnetic wave with "decreased" phase velocity $c/n \times \sin\varphi$ propagates in a gap between a total-internal reflection prism and the investigated sample (n is the refractive index of the prism). This wave corresponds to the dashed line of Fig. 12, which crosses the dispersion curves of the surface oscillations, thereby ensuring the possibility of direct interaction of the light with the surface phonons. Minima appear in the reflection spectrum $R = I(\omega)/I_0(\omega)$, and their positions are determined by the frequencies of the surface phonons at the given q_x. The value of q_x is connected with the incidence angle of the light: $q_x = (\omega/c)n \sin\varphi$. Variation of φ makes it possible to plot the dispersion curves $\omega(q_x)$. The incident light wave is polarized in the incidence plane (p polarization). No interaction with the surface waves was observed for s polarization, owing to the polarization of the surface waves (see Chap. 2).

Figure 14 shows the dispersion curves for a thick (semi-infinite) NaCl crystal[104]. A comparison of curves 1 and 2 in Fig. 14 illustrates clearly the dependence of the surface frequencies on ϵ_M.

Calculation of the PTIR spectra and of the dispersion curves for NCl and other alkali-halide crystals, with a function $\epsilon(\omega)$ that includes the frequency-dependent damping constant $\Gamma(\omega)$ (but without allowance for the anharmonic shift $\Delta(\omega)$) has led to a certain disparity with the experimentally measured frequencies, reaching 15–30 cm^{-1} for various crystals. Thus, for NaCl at $\varphi = 48^\circ$, the calculated and measured values are 234 and 215 cm, respectively. In[104], a two-pole approximation was used for $\epsilon(\omega)$ in NaCl, with an additional pole at

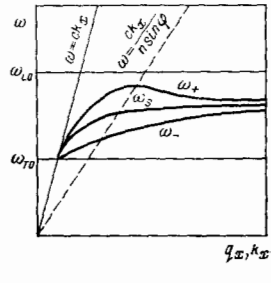

FIG. 12. Dispersion curves of surface oscillations ω_+ and ω_- for a thin film and ω_s for a semi-infinite crystal. The dashed line corresponds to the light wave in the PTIR method. Light absorption takes place at the frequencies corresponding to the points of intersection of this line with the surface modes.

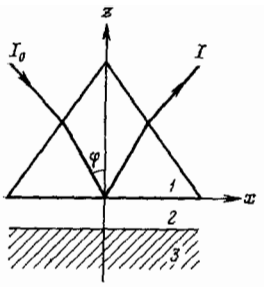

FIG. 13

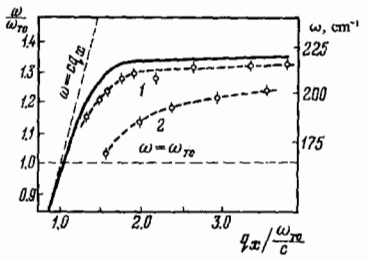

FIG. 14

FIG. 13. Geometry of experiment aimed at observing surface modes by the PTIR method. 1—Silicon prism, 2—gap (vacuum or non-absorbing dielectric), 3—investigated crystal, $R(\omega) = I(\omega)/I_0(\omega)$.

FIG. 14. Dispersion curves of surface oscillations for a "semi-infinite" NaCl crystal [104]. 1—Vacuum gap between prism and samples ($\epsilon_M = 1$) (solid curve—calculation); 2—gap filled with paraffin ($\epsilon_M = 1.96$).

247 cm^{-1}. Using this approximation, which to a certain degree takes into account not only the damping but also the anharmonic shift, the discrepancy between theory and experiment does not exceed 4—5 cm^{-1} (see Fig. 14). Perhaps more consistent is allowance for anharmonicity and the use of $\epsilon(\omega)$ in the form (5.3), which explicitly includes the functions $\Gamma(\omega)$ and $\Delta(\omega)$. This was done in[89] using the experimentally determined $\Gamma(\omega)$ and $\Delta(\omega)$, and the agreement with the experimental data was excellent[104]. Good agreement between theory and experiment was noted also in an investigation of surface modes in plates of a number of other crystals, CaF_2, CdF_2[104], GaP[105] (Fig. 15) and $CaMoO_4$[106]. In the above-mentioned cases, the experimental values of ω_S were close to the calculation results even in the harmonic approximation, i.e., the anharmonic corrections were small. For NaF, to the contrary, a noticeable contribution of anharmonic corrections was noted in[186] in accord with[104]. A certain discrepancy (~10 cm^{-1}) between the calculated harmonic and experimental values of ω_S was obtained also in measurements performed in SiC[187].

A splitting of the peak in the PTIR spectrum was observed with decreasing plate thickness, corresponding to the presence of two surface modes ω_+ and ω_- (cf. Fig. 12). Surface oscillations in a polycrystalline NaCl film 2 μ thick was investigated in greater detail by the PTIR method in[107]. The film was deposited by vacuum evaporation on a polyethylene substrate. The gap between the prism and the film was filled with paraffin. The PTIR spectrum were calculated for such a sandwich. Fig. 16 shows the PTIR spectra of an NaCl film for three angles of incidence, i.e., three values of q_x. The strongest peaks in the spectrum correspond to two surface-oscillation branches. The dispersion curves constructed from the positions of the minima in the PTIR spectra at different incidence angles are compared in Fig. 17 with the calculated relations. The discrepancy between the theoretical and experimental values of the frequencies lies in the range 5—10 cm^{-1}, i.e., not much larger than for a "semi-infinite" crystal with the same form of $\epsilon(\omega)$. The experimental spectrum (Fig. 16a) shows a singularity in the low-frequency region at $\omega \sim \omega_{TO}$. This additional peak is interpreted in[107] as a result of interaction of the light with the nonradiative polariton modes located in the region L_1 on the $(\omega - q_x)$ plane (see Fig. 1).

Thus, the use of the PTIR method has made it possible to investigate in detail the dispersion curves of pure

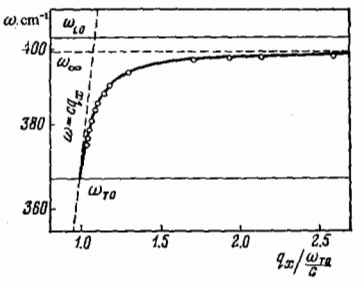

FIG. 15

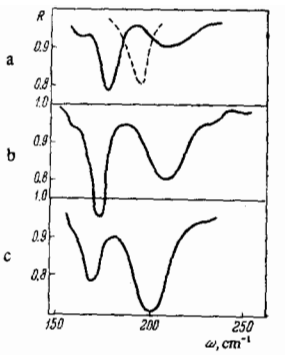

FIG. 16

FIG. 15. Dispersion curve of surface oscillations for a "semi-infinite" GaP crystal [105]. Solid curve—calculation, circles—experiment.

FIG. 16. PTIR spectra for NaCl film 2μ thick with $\varphi = 56°$ (a), 36° (b), and 31° (c) [107]. The dashed lines shows the position of the saturated peak in the spectrum of the "semi-infinite" crystal.

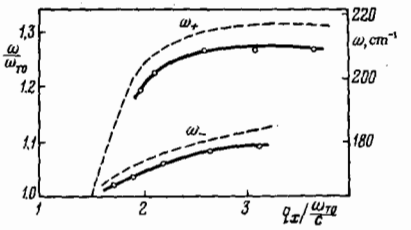

FIG. 17. Dispersion curves of surface oscillations in an NaCl film 2μ thick [107]. Solid curves—experiment, dashed—calculation.

surface modes both in a plate and in a thin film, and also to observe the exchange polariton modes in the nonradiative region of the spectrum. The result of these investigations have shown, in particular, that if the frequency-dependent complex $\epsilon(\omega)$ is known with sufficient accuracy the position of the surface frequencies of the SO-I type can be predicted with good accuracy from phenomenological calculations. On the other hand, the noticeable sensitivity of ω_S to the values of $\epsilon(\omega)$ makes it possible, in principle, to use measurements of the surface frequencies to solve the inverse problem, i.e., to determine the optical constants of crystals. We note in this connection that, at least for alkali-halide crystals and probably for many others, the position of the surface frequencies is practically independent of the damping $\Gamma(\omega)$ at realistic (i.e., comparable with the widths of the bands observed in the spectrum) values of $\Gamma(\omega)$ for the given frequency range and, to the contrary, is very sensitive to the anharmonic shift $\Delta(\omega)$. This circumstance suggests a relatively simple method of determining the frequency dependence of $\Delta(\omega)$.

One of the modes of the surface oscillations (ω_-) was recently observed in Raman-scattering spectra of a thin (2500 Å) GaAs film epitaxially grown on a sapphire substrate[188] (see also the calculation in[189]). The scattering was observed at small angles (1—12°) in a "transmission" geometry, with excitation by an argon laser (4880 Å).

In anisotropic crystals, the surface modes should have a number of interesting features[15,108,109]. The dispersion relations for a semi-infinite anisotropy crystal, obtained in[108,109], can be expressed in the following form, which facilitates the analysis:

$$\varepsilon_x = -\left\{\frac{(\varepsilon_x/\varepsilon_z)\left[(c^2q_x^2/\omega^2) - \varepsilon_z\right]}{(c^2q_x^2/\omega^2) - 1}\right\}^{1/2}. \qquad (6.1)$$

It is assumed here that the z axis is normal to the

crystal surface ($q_y = 0$), and the dielectric tensor is diagonal in the axes x, y, and z. At $\epsilon_x = \epsilon_z$ Eq. (6.1) goes over, naturally, into the dispersion relation for an isotropic crystal.

It follows from (6.1) that the surface modes of the oscillations can exist in two cases: 1) $\epsilon_x < 0$, $\epsilon_z < 0$; 2) $\epsilon_x < 0$, $(q_x/(\omega/c))^2 < \epsilon_z$. In the first case the surface modes are preserved also at large q_x and can be obtained by theoretical analysis of the problem without considering retardation, allowance for which merely deforms their dispersion curve in the region of small q_x. In this sense they are analogous to the previously considered surface modes in an isotropic crystal. In the second case, the surface oscillations exist only at sufficiently small q_x. This mode has a pure polariton character and has no analog in isotropic crystals. Experimentally, these two surface-oscillation modes were observed[110] in uniaxial MgF_2 crystals with rutile structure. For an MgF_2 plate cut in such a way that the fourfold axis C_4 is perpendicular to the plane of the plate ($C_4 \parallel Oz$), a polariton branch was observed in the region 250–300 cm^{-1}, i.e., in the region of dipole resonance polarized perpendicular to C_4 (in this case $\epsilon_x = \epsilon_\perp < 0$, but $\epsilon_z = \epsilon_\parallel > 0$), and in a limited interval of small q_x (Fig. 18a). When q_x becomes equal to $(\omega/c)\sqrt{\epsilon_z}$, i.e., the phase velocity of the surface wave becomes comparable with the phase velocity $c/\sqrt{\epsilon_z}$ of the volume polariton, strong radiative broadening sets in. At this point $\epsilon_x = 0$ in accord with (6.1), i.e., the point of intersection of the dispersion curves of the surface and volume polaritons corresponds to the frequency of the longitudinal phonon propagating along the Ox axis. The minimum in the PTIR spectrum then vanishes. When C_4 lies in the plane of the plate and is parallel to the Oy axis, we have $\epsilon_x = \epsilon_z \equiv \epsilon_\perp < 0$. Surface phonons of the ordinary type were observed in this case in the entire investigated interval of q_x (Fig. 18b). The dispersion curves for the same orientations are shown in Fig. 19. At $C_4 \parallel Ox$ we have $\epsilon_x = \epsilon_\parallel > 0$, and no surface waves are produced even though $\epsilon_x = \epsilon_y < 0$.

The spectrum of the surface phonons in α-quartz was recently investigated in detail in a number of studies[190]. In view of the complexity of the volume vibrational spectrum of α-SiO_2, the surface-phonon spectrum is also very rich: it contains a large number of dispersion modes of both the first and of the second type in accordance with (6.1).

From among the few studies of the manifestations of surface phonons in transport phenomena, we note the observation of frequency oscillations of the photoconductivity of ZnO, with a period equal to the surface-phonon frequency[191]. The observed effect is obviously due to scattering of hot electrons with emission of surface phonons.

7. INTERACTION OF SURFACE PHONONS WITH SURFACE PLASMONS. MIXED PLASMON-PHONON SURFACE MODES

The investigation of surface plasmons in metals has been the subject of many theoretical as well as experimental studies. In Chap. 2 above we referred to some of them. Surface plasmons were recently investigated also in semiconductors: in[111] they plotted the surface-plasmon dispersion curve for InSb.[15)] The electron concentration exceeded 10^{18} cm^{-3}, so that the greater part of the dispersion curve for the plasmons was located

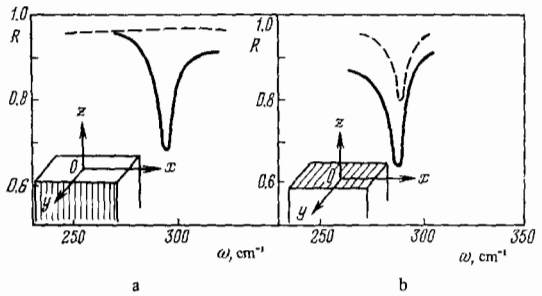

FIG. 18. Orientation of MgF_2 crystals in the experiment aimed at observing surface oscillations and the PTIR spectra [110]. a) $C_4 \parallel Oz$, b) $C_4 \parallel Oy$. The direction of the C_4 axis is shown hatched. $q_x c/\omega$ is equal to 1.98 and 1.85 for the solid and dashed curves, respectively; the last figure exceeds $\sqrt{\epsilon_z}$ in this region ($\sqrt{\epsilon_z} \approx 2.8$), i.e., $\omega/q_x < c/\sqrt{\epsilon_z}$.

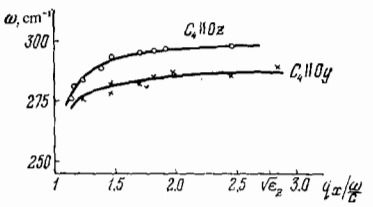

FIG. 19. Dispersion relations of surface modes in MgF_2 crystals [110]. The abscissas represent the values of $q_x c/\omega = \sqrt{\epsilon_z}$ at which the surface waves vanish at the orientation $C_4 \parallel Oz$.

above the region of the phonon frequencies. However, if the frequencies of the surface plasmons and of the surface phonons turned out to be close, then one can expect the formation of mixed plasma-phonon surface modes[113–115]. This effect was indeed observed in[116,117][16)].

We assume that the contributions of the phonons and plasmons to the dielectric constant are additive. In the long-wave limit, when $qv_F \ll \omega$ (v_F is the velocity on the Fermi surface), i.e., when there is no static screening of the long-range forces by the conduction electrons, and neglecting damping, we have

$$\varepsilon(\omega) = \varepsilon_\infty + \frac{\varepsilon_0 - \varepsilon_\infty}{1 - (\omega/\omega_{TO})^2} - \frac{\omega_p^2}{\omega^2}, \qquad (7.1)$$

where $\omega_p = (4\pi ne^2/m^*)^{1/2}$ is the plasma frequency and m^* is the effective mass.

The solution (7.1) for $\epsilon = 0$ yields the well known mixed "volume" longitudinal modes[119,120]. A joint solution of (7.1) and (2.13) yields the dispersion and concentration dependences of the surface plasma-phonon modes. The results of these calculations are compared in[116] with the experimental data obtained by the PTIR method with InSb plates at n from 10^{16} to 10^{18} cm^{-3}, i.e., precisely in the range in which the frequency of the surface plasma oscillations is close to the frequency of the surface phonons (about 190 cm^{-1})[17)]. Figure 20 shows the dependence of the frequencies of the surface plasmon-phonon modes on the carrier density. In the absence of interaction, the plasmon and phonon modes intersect. The interaction lifts the degeneracy. In the vicinity of the intersection point, the modes acquire a mixed character. At low densities, the lower branch is plasmon-like and the upper phonon-like, and at higher densities the situation is reversed. In[117] we also obtained dispersion relations for mixed plasmon-phonon modes and investigated their damping. The half-width of the peak in the PTIR spectrum, corresponding to the surface phonon in undoped InSb, was 3 cm^{-1}, which

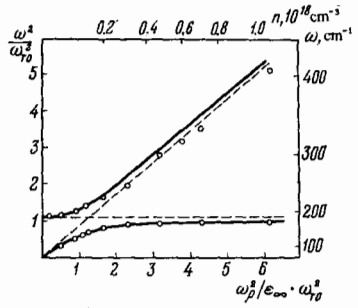

FIG. 20. Dependence of the frequencies of plasmon-phonon surface modes on the free-carrier concentration n or on $\omega_p^2 = 4\pi ne^2/m^*$ in InSb [116]. The curves were obtained by the PTIR method: $\varphi = 23°$, $q_x = (\omega/c)n \sin\varphi$. Solid curves–calculation, circles–experiment, dashed curves–"bare" plasmon and phonon branches (without interaction).

is close to the damping of volume phonons. However, in the plasma region of the dispersion curves the widths of the peaks are several times larger than the corresponding values for the volume excitations. The reason for this additional broadening of the surface-plasmon peak, i.e., for the increase in the rate of their decay is still unclear. The exponentially damped amplitude of the surface excitations contains, generally speaking, harmonics with arbitrarily large q, including those close to the limiting Fermi momentum, and this can lead to a broadening due to the Landau damping[121]. In the considered case of long waves however, the corresponding contribution can apparently be neglected. Another additional damping mechanism may be connected with the presence of a surface barrier (there is usually a depleted layer on the n-InSb surface[122]). In such a plasma with inhomogeneous concentration there can occur an enhanced transfer of surface-plasmon energy to that of volume plasmons[123]. In any case, this interesting question calls for further research, both theoretical and experimental (the influence of the surface potential, of surface scattering, etc.).

The energy-spectrum of a system of coupled phonon-plasmon surface modes becomes more complicated in an external magnetic field if the cyclotron frequency ω_c is close to the surface-excitation frequencies. A theoretical investigation of this question was recently carried out in[124,192] (see also[113]). The calculated dispersion curves contain many additional singularities that appear when the magnetic field is turned on (for example, gaps appear in the energy spectrum of the surface modes, the positive and negative directions of q_x become nonequivalent at $H \parallel q_x$). At $\omega_c > \omega TO$ a new surface mode is produced, located between ωTO and ωLO and having a pure phonon character. The appearance of such a mode with small damping was recently observed in InSb at H = 43 kG[193]. Even in weaker fields, a broadening of the peaks in the PTIR spectra, due to the intersection of the surface modes with the volume spectrum, was observed in[193].

Mixed plasmon-phonon modes in minute crystals were considered in[194]. In this geometry, just as surface phonons, they turn out to be radiative and are observed in the infrared absorption spectra[195].

8. CONCLUSION

In the concluding part of the review we shall describe briefly some other types of surface waves in solids and compare the degree of the understanding of the problem with that of surface phonons. Naturally, the corresponding bibliography will not be as complete as in the main part of the review.

a) Surface plasmons in metals[18] The presence of the boundary leads to the appearance of surface plasmons (SP) in the plasmon spectrum. Since the interaction in the plasma is long-range, SP of the SO-I appear in the spectrum (SO-II modes in a plasma have not been discussed). The first theoretical investigation of SP[8,9,35,36] were carried out by a phenomenological approach using the same methods as for surface phonons (see Chap. 2). The dispersion dependence of the SP frequency ω_{sp} on the dimensionless parameters $q_\perp L$ and $q_\perp c/\omega_p$ was obtained[9,36]. A study was initiated recently of the dependence of ω_{sp} on a third dimensionless parameter $q_\perp k_F$, where $\hbar k_F$ is the Fermi quasimomentum. For metals we have $k_F \sim 1/a$, so that this problem is related to the study of the frequency dispersion of surface phonons with respect to $q_\perp a$, and the construction of the corresponding theory calls for the use of a microscopic approach, different methods being employed: a) hydrodynamic equations of motion for a charged liquid[125,126]; b) random-phase approximation[127-129]; c) self-consistent field approximation[130]; d) Boltzmann equation and the system of Maxwell's equations[131-133] (see also[134,135]). At $q_\perp/k_F \ll 1$ (but $q_\perp L \to \infty$ and $q_\perp c/\omega_p \to \infty$), the following was obtained:

$$\omega_{sp}(q_\perp/k_F) \approx \omega_{sp}(0)\,[1 + (A_1 + iA_2)\, q_\perp/k_F]. \qquad (8.1)$$

The numerical values of A_1 and A_2, and even the sign of A_1, depend strongly on the microscopic model of the surface (the form of the potential at the boundary or of the electron density[125-130]). We note that this situation is similar to the influence of SO-II in phonon spectra on the dispersion of the SO-I modes with respect to the parameter $q_\perp a$. In particular, for electrons specularly reflected from the surface, the following dispersion equation was obtained in[131] ($q_\perp L \to \infty$, $q_\perp c/\omega_p \to \infty$):

$$-1 = \frac{2q_\perp}{\pi}\int_0^\infty \frac{dq_z}{(q_z^2 + q_\perp^2)\,\varepsilon(q,\omega)}, \qquad (8.2)$$

and reduces at small $q_\perp/k_F$ to the form

$$1 + \varepsilon^{-1}(0,\omega) = \frac{q_\perp}{4\pi}\int_{-\infty}^{\infty} dq_z \left(\frac{q_z}{2}\right)^{-2} [\varepsilon^{-1}(0,\omega) - \varepsilon^{-1}(q,\omega)]. \qquad (8.3)$$

If we let $c \to \infty$ and $L \to \infty$ in (3.8) we obtain a formula similar to (8.3). The difference in the integration limits is due to the finite character of the Brillouin zone, and the presence of $a^2[\sin(aq_z/2)]^{-2}$ in (3.8) in place of $(q_z/2)^{-2}$ is due to the periodicity of the lattice. An expression of the type (8.3) with allowance for retardation has been obtained in[133], and can be reduced, with analogous stipulations, to the form (3.8). The condition of specular reflection from the surface is equivalent to ignoring the role of SO-II in the theory of surface phonons, so that the obtained dispersion relations are quite similar. The microstructure of the surface and its imperfection are usually taken into account in the boundary conditions for the reflection of the electrons from the surface (the fraction of diffuseness). Obviously, this is a poor approach if the typical dimensions of the roughnesses on the surface are comparable with the characteristic length over which the amplitudes of the SP attenuates.

Surface plasmons were first observed in the investigation of the characteristic losses of fast electrons passing through a metallic foil[136], and the radiation predicted in[9], which occurs when radiative surface plasmons generated when a foil is bombarded by fast

electrons (particular case of transition radiation[138]) was later observed in[10,137]. Similar radiation is produced also when bulky samples with non-ideal surfaces are bombarded with electrons (natural roughness, artificially produced grating), owing to the decay of the nonradiative (tangential) surface plasmons[139-141].

Recent studies of elastic (ELEED) and inelastic (ILEED) diffraction of slow electrons have uncovered new possibilities for the investigation of SP. Thus, in[142] an attempt was made to reconstruct the dispersion relations and the damping at $q_\perp > 10^5\ cm^{-1}$ from ILEED data. The interpretation of the angular dependences and of the absolute values of the intensities of the reflected beams was based on a microscopic approach (see, e.g.,[130,143], where an extensive list of references is given), since it is impossible to describe fully all these effects within the framework of the phenomenological theory[8].

Direct optical excitation of SP was effected by various methods. One of them, the PTIR method[102a], was already discussed in Chap. 6. Other methods are based on the fact that the interaction of the nonradiative SP with the radiation field can be effected on a nonideal surface[112 144-146]. The reflection coefficient has a dip near $\omega_p/\sqrt{2}$[147], the depth of which depends strongly on the quality of the surface. Illumination of a nonideal surface excites SP that decay and emit light[144,148,149]. An analogous effect is observed upon illumination of a smooth surface on which a diffraction grating is produced[112]. The spectral dependence of the photoemission produced by illumination of a nonideal surface has a clearly pronounced maximum near $\omega_p/\sqrt{2}$.[150]

In the tunnel effect, SP produce a hump on the d^2I/dV^2 plot against V near $eV_{max} = \hbar\omega_p\sqrt{2}$[151] (see[152] for the theory). These experiments can yield the value of Im $\omega_{sp}(q_\perp)$, which turns out to be 10—20 times larger than the theoretical value. We note that to describe many of these phenomena it is necessary to know the Hamiltonian of the interaction of the electrons with the SP (see, e.g.,[153]).

b) **Surface magnons (SM).** They are produced in the magnon spectrum of ferromagnetic and antiferromagnetic crystals in the presence of a boundary. As in the case of phonon spectra, the boundary causes the appearance of SM that decrease slowly in amplitude away from the surface—SO-I (magnetostatic surface modes) and microscopic surface modes of the SO-II type. Modes of SO-I type, which are due to the long-range magnetic dipole interaction, can be described in the phenomenological approach, the calculation method being reminescent in many respect of that developed in Chap. 2 for surface phonons. SM of the SO-I type were obtained in connection with a study of ferromagnetic and antiferromagnetic resonances in an ellipsoid[39] and in a plate[40] (see also[154]). The influence exerted on the SO-I by their intersection with the volume-magnon spectrum was recently calculated in[155,156]. The calculations were performed with the aid of magnetostatics with allowance for weak spatial dispersion. Although the same procedure is used in both papers, the conclusions of the authors are different. It is stated in[156] that the SO-I of ferromagnets vanish when the spatial dispersion is taken into account. It seems to be more consistent to speak of a broadening of the SO-I lines as a result of the intersection with the volume magnon spectrum[155] (compare with the analogous situation for surface phonons, as described in Chap. 3). Although the qualitative conclusions concerning the influence of the intersection of the SO-I with the continuous spectrum are correct, nevertheless, as emphasized in Chap. 3, the phenomenological approach with allowance for weak spatial dispersion can hardly yield good guantitative results, since we are dealing here, generally speaking, with intersection with the shortwave part of the volume spectrum. In particular, this method cannot be used to obtain the sharp increase of the line width near the van Hove singularities in the spectrum. An extensive bibliography on SM can be found in[157].

Besides SO-I, a study was also made of SO-II (see, e.g.,[158-160]) which appear in the magnon spectrum as a result of perturbation of the exchange-interaction forces near the surface. Since this interaction has a short-range character, the surface perturbation subtends over only several surface atomic layers, and the calculation can be carried out with the aid of the standard Green's function method[3], initially developed for the calculation of the SO-II levels in phonon spectrum.

At present there is no unified microscopic theory for SM, within which SM of both types can be obtained in analogy with the result for phonon spectra. Allowance for the influence of the exchange-interaction forces on the SO-I spectrum within the framework of the phenomenological approach, with weak spatial dispersion taken into account (see, e.g.,[161]) calls in our opinion, for the reasons cited above, for an additional justification. Since the Hamiltonian that describes the magnon waves in an infinite crystal is known in the entire wave-vector range (see, e.g.,[154]), such a microscopic theory can be constructed by the same methods as were used to calculate surface phonons (see Chap. 3).

We note that one usually deals with low-frequency SM. On the other hand, high-frequency SM, which can be investigated by optical methods, exist in antiferromagnets and ferrimagnets.

c) **Surface excitons (SE).** Surface states are produced also in molecular crystals. Since the Hamiltonian describing a molecular crystal contains, generally speaking, both a long-range contribution from the dipole-dipole interaction and a contribution from the short-range forces, this situation is quite similar to that encountered by us in the analysis of surface phonons in ionic crystals and SM. A theoretical microscopic investigation of SE was carried out in[162-165], with only the interaction with the nearest neighbors taken into account in[162,163], and the long-range Coulomb contribution completely ignored, so that only SE of the SO-II type could be considered. In[164,165] the SE spectra were calculated with allowance for the dipole-dipole interaction forces, but a transition to the continual approximation was used from the very beginning in the Hamiltonian, so that it was impossible to describe in a unified manner the SE of both types. A phenomenological theory for SE of the SO-I type was developed in[2], where the unity of the surface excitations of the type SO-I in polarizable media was emphasized. A phenomenological theory with allowance for weak spatial dispersion, developed in[2,15], made possible a considerable step forward in the study of surface excitations in polarizing media. In particular, a study was made of SE of SO-I type, for which $\mathbf{E} = 0$ but $\mathbf{D} \neq 0$, called surface polarization waves, which can be obtained only when account is taken of spatial dispersion and addi-

tional boundary conditions are used for Maxwell's equations. From among the recent theoretical results, we note the study of SE on the boundary between a molecular crystal and a metal[38], where new surface states are produced in the spectrum. The interaction of SE with light was studied in[166], starting with an experimental investigation of SE. In particular, it was noted that SE exert an influence on the spectra of light reflection from the surface of a molecular crystal[167] and on the luminescence spectra[168] in these crystals.

Among other types of surface excitations, we point to surface piezoacoustic waves in piezoelectrics[169-171], and also surface helicons in conducting crystals[172].

[1)] In addition, adsorbed atoms can be present on the surface and can make their own contribution to the surface-excitation spectrum. We shall, however, neglect this circumstance and discuss only chemically pure surfaces.

[2)] Surface plasmons have by now been sufficiently well investigated both theoretically and experimentally, and the pertinent bibliography contains hundreds of papers (see, e.g., the review [10] and also Chap. 8 of the present article).

[3)] There seems to be an error in [44] (see [45]).

[4)] Similar methods were used in [60-62] to calculate the spectra in nonionic crystal plates.

[5)] According to [19], the low-frequency surface modes on Fig. 4 decrease rapidly in amplitude and pertain to SO-II.

[6)] The intervals of $q_\perp$ used in the calculations of [19] were too large, so that it was impossible to observe the mode repulsion at small $q_\perp$, inasmuch as at N = 15 the region where the SO-I have a strong dispersion is of the order of 1/15 of the value of $q_\perp$ at the boundary of the Brillouin zone.

[7)] When the interaction with the more remote neighbors is taken into account, the order of the determinant increases as a result of the appearance of additional variables that come from the contributions of the type $A''_{\alpha\beta}(^{q}_{k,k'})\exp(2iq'_z a)$ etc. to Λ.

[8)] This result follows directly from (3.6) if the term integral in q_z is discarded and the matrix $\bar{C}$ is replaced by its long-wave limit.

[9)] The quantity q_z in a plate (normal along the z axis), which enters in expression (38) of [73], is not a wave vector in the true sense of the word. In particular, the momentum conservation law is not satisfied for q_z in the case of interaction with a free electron, owing to the absence of spatial homogeneity along the z axis. However, in analogy with the case of an infinite crystal, $q_z = 2\pi n/L$, n = 0, 1, 2, ..., N-1.

[10)] More accurately, one should write $|\epsilon_\perp(\omega)\epsilon_\parallel(\omega)| = 1$, where both $\epsilon_\perp$ and $\epsilon_\parallel$ should be negative. For a detailed analysis for anisotropic crystals see Chap. 6.

[11)] In [78] they considered, in addition to ionic crystals, also the case of homopolar crystals (silicon). The diffraction of electrons reflected from the surface of silicon was experimentally investigated in [79].

[12)] In [84], the band near ω_{TO} was present in the transmission spectrum of KBr alongside the surface band up to $d \sim 0.3\mu$. The reason for this disagreement with the theory was not explained.

[13)] This distinguishing feature is completely neglected in certain most recent works on the dynamics of ionic crystals [99]. The frequencies of the minima in the transparency spectra of powders of a number of crystals (CaF_2, MgO, ZnS) receive a patently incorrect interpretation by the authors of these papers.

[14)] The method proposed in [102] differs from the usual PTIR procedure [103] in the presence of a gap between the prism and the investigated crystal. This plays an important role in the investigation of nonradiative modes. The size of the gap in the experiment should be large enough to reduce to a minimum the perturbing action of the prism on the surface-mode characteristics (for details see [104]). This fact, which is of importance for the experimental procedure, is analyzed in [185] by means of a response function introduced there for the surface modes.

[15)] In analogy with surface phonons, surface plasmons in a plate are nonradiative and therefore do not interact directly with light on a smooth surface. In [111] and in some other studies of surface plasmons (see, for example, [112]) a periodic grating was deposited on the surface of the sample, with a distance d between the lines (grooves). Then the condition for momentum conservation in interaction with light takes the form $q_x = (\omega/c)\sin\varphi + n(2\pi/d)$ (n is an integer), i.e., the momentum is conserved accurate to the "reciprocal lattice vector."

[16)] It appears that some manifestations of the interaction of surface plasmons with phonons were observed in [118], but the imperfect experimental procedure made the interpretation of the results obtained there difficult.

[17)] The width of the dispersion of the surface phonons in InSb is small because ω_{TO} is close to ω_{LO} (i.e., ϵ_0 is close to ϵ_∞), and amounts to only 10 cm^{-1}.

[18)] Certain investigations for SP in semiconductors are described in Chap. 7.

[1] M. Born and K. Huang, Dynamical Theory of Crystal Lattices, Oxford U. Press, 1954.
[2] V. M. Arganovich and V. L. Ginzburg, Kristallooptika s uchetom prostranstvennoĭ dispersii i teoriya éksitonov (Spatial Dispersion in Crystal Optics and the Theory of Excitons), Moscow, Nauka (1965) [Wiley, 1966].
[3] I. M. Lifshitz and A. N. Rozentsveĭg, Zh. Eksp. Teor. Fiz. 18, 1012 (1948).
[4] I. M. Lifshitz and S. I. Pekar, Usp. Fiz. Nauk 56, 531 (1955).
[5] L. D. Landau and E. M. Lifshitz, Teoriya uprugosti (Theory of Elasticity) Nauka, 1965 [Addison-Wesley, 1971].
[6] R. M. White, Proc. IEEE 58, 1238 (1970).
[7] A. Maradudin, Defects and Vibrational Spectra of Crystals (Russ. transl.), Mir, 1968.
[8] R. H. Ritchie, Phys. Rev. 106, 874 (1957).
[9] R. A. Ferrell, ibid. 111, 1214 (1958).
[10] W. Steinman, Phys. Stat. Sol. 28, 437 (1968).
[11] D. W. Berreman, Phys. Rev. 130, 855 (1963).
[12] R. Fuchs and K. L. Kliewer, ibid. A140, 2076 (1965).
[13] K. L. Kliewer and R. Fuchs, ibid. 144, 495 (1966).
[14] K. L. Kliewer and R. Fuchs, ibid. 150, 573.
[15] V. M. Agranovich, Teoriya eksitonov (Exciton Theory) Nauka, 1968.
[16] V. V. Bryksin and Yu. A. Firsov, Fiz. Tverd. Tela 11, 2167 (1969) [Sov. Phys.-Solid State 11, 1751 (1970)].
[17] V. V. Bryksin and Yu. A. Firsov, Fiz. Tverd. Tela 14, 1148 (1972) [Sov. Phys.-Solid State 14, 981 (1972)].
[18] A. A. Lucas, J. Chem. Phys. 48, 3156 (1968).
[19] S. Y. Tong and A. A. Maradudin, Phys. Rev. 181, 1318 (1969).
[20] H. Böersch, J. Geiger, and W. Stickel, Phys. Rev. Lett. 17, 379 (1966).
[21] T. P. Martin, Phys. Rev. 177, 1349 (969).
[22] J. T. Luxon and R. Summit, J. Chem. Phys. 50, 1366 (1969).
[23] J. Pastrňák and B. Hejda, Phys. Lett. A29, 314 (1969); Phys. Stat. Sol. b35, 941 (1969).
[24] V. V. Bryksin, Yu. M. Gerbshteĭn, and D. N. Mirlin, Fiz. Tverd. Tela 13, 2125 (1971) [Sov. Phys.-Solid State 13, 1779 (1972)].
[25] L. D. Landau and E. M. Lifshits, Elektrodinamika sploshnykh sred (Electrodynamics of Continuous Media) Fizmatgiz, 1959 [Pergamon, 1959].
[26] H. Fröhlich, Theory of Dielectrics, Oxford U. Press, 1958.
[27] R. Fuchs, K. L. Kliewer, and W. J. Pardee, Phys. Rev. 150, 589 (1966).
[28] R. Englman and R. Ruppin, Phys. Rev. Lett. 16, 898 (1966).
[29] R. Fuchs and K. L. Kliewer, J. Opt. Soc. Am. 58, 319 (1968).
[30] R. Englman and R. Ruppin, J. Phys. C1, 614 (1968).
[31] R. Englman and R. Ruppin, ibid., p. 630.
[32] R. Englman and R. Ruppin, ibid., p. 1515.
[33] R. Ruppin and R. Englman, Rept. Progr. Phys. 33, 149 (1970).

[34] L. Dobrzynski and A. A. Maradudin, Phys. Rev. B6, 3810 (1972).
[35] F. A. Stern and R. A. Ferrell, ibid. 120, 130 (1960).
[36] R. H. Ritchie and H. B. Eldridge, ibid. 126, 1935 (1962).
[37] V. M. Agranovich and V. L. Ginzburg, Zh. Eksp. Teor. Fiz. 61, 1243 (1971) [Sov. Phys.-JETP 34, 662 (1972)].
[38] V. M. Agranovich, A. G. Mal'shukov, and M. A. Mekhtiev, Fiz. Tverd. Tela 14, 849 (1972) [Sov. Phys.-Solid State 14, 725 (1972)].
[39] L. R. Walker, Phys. Rev. 105, 390 (1957).
[40] J. Eshbach and R. Damon, ibid. 118, 1208 (1960); J. Phys. Chem. Sol. 19, 308 (1961).
[41] P. M. Morse and H. Feshbach, Methods of Theoretical Physics, Vol. II, McGraw, 1953.
[42] H. Bilz, L. Genzel, and H. Happ, Zs. Phys. 160, 535 (1960).
[43] G. Mie, Ann. d. Phys. (Lpz.) 25, 377 (1908).
[44] B. N. N. Achar and G. R. Barsch, Phys. Rev. 188, 1356, 1361 (1969).
[45] T. S. Chen, R. E. Allen, G. P. Alldredge, and F. W. de Wette, Sol. State Comm. 8, 2105 (1970).
[46] T. S. Chen, G. P. Alldredge, F. W. de Wette, and R. E. Allen, Phys. Rev. Lett. 26, 1543 (1971).
[47] T. S. Chen, G. P. Alldredge, F. W. de Wette, and R. E. Allen, Phys. Rev. B6, 623 (1972).
[48] T. S. Chen, G. P. Alldredge, F. W. de Wette, and R. E. Allen, ibid., p. 627.
[49] T. S. Chen, G. P. Alldredge, F. W. de Wette, and R. E. Allen, J. Chem. Phys. 55, 3121 (1971).
[50] T. S. Chen, G. P. Alldredge, and F. W. de Wette, Sol. State Comm. 10, 941 (1972).
[51] T. S. Chen, G. P. Alldredge, and F. W. de Wette, Phys. Lett. A40, 401 (1972).
[52] W. E. Jones and R. Fuchs, Phys. Rev. B4, 3581 (1971).
[53] K. B. Tolpygo, Tr. IF AN USSR 6, 102 (1955).
[54] V. V. Bryksin and Yu. A. Firsov, Zh. Eksp. Teor. Fiz. 56, 841 (1969) [Sov. Phys.-JETP 29, 457 (1969)].
[55] H. B. Rosenstock, Phys. Rev. 121, 416 (1961).
[56] A. A. Maradudin and G. H. Weiss, ibid. 123, 1968.
[57] A. A. Lucas, ibid. 162, 801 (1967).
[58] H. B. Rosenstock, ibid. A136, A761 (1964).
[59] T. Barron, ibid. 123, 1995 (1961).
[60] R. E. Allen, G. P. Alldredge, and F. W. de Wette, ibid. B4, 1648, 1661, 1682 (1971).
[61] R. E. Allen, G. P. Alldredge, and F. W. de Wette, ibid. B6, 632 (1972).
[62] G. P. Alldredge, R. E. Allen, and F. W. de Wette, J. Ac. Soc. Am. 49, 1453 (1971).
[63] L. Genzel and T. P. Martin, Phys. Stat. Sol. b51, 101 (1972).
[64] Yu. M. Kagan and Ya. A. Iosilevskiĭ, Zh. Eksp. Teor. Fiz. 42, 259 (1962) [Sov. Phys.-JETP 15, 182 (1962)].
[65] L. I. Korovin and S. T. Pavlov, Zh. Eksp. Teor. Fiz. 53, 1708 (1967); 55, 349 (1968) [Sov. Phys.-JETP 26, 979 (1968); 28, 183 (1969)].
[66] H. Böersch, J. Geiger, and W. Stickel, Zs. Phys. 212, 130 (1968).
[67] H. Ibach, Phys. Rev. Lett. 24, 1416 (1970).
[68] M. Hattori and K. Yamada, J. Phys. Soc. Jap. 18, 200 (1963).
[69] T. Fujiwara and K. Othaka, ibid. 24, 1326 (1968).
[70] A. A. Lucas and E. Kartheuser, Phys. Rev. B1, 3588 (1970); I. B. Chase and K. L. Kliewer, ibid. B2, 4389.
[71] A. A. Lucas, E. Kartheuser, and R. G. Badro, ibid., p. 2488.
[72] A. A. Lucas, E. Kartheuser, and R. G. Badro, Sol. State Comm. 8, 1075 (1970).
[73] V. V. Bryksin and Yu. A. Firsov, Fiz. Tverd. Tela 13, 496 (1971) [Sov. Phys.-Solid State 13, 398 (1971)].
[74] J. Ziman, Electrons and Phonons, Oxford, 1960; Russ. Transl., IIL, 1962, p. 197.
[75] M. Šunjić and A. A. Lucas, Phys. Rev. B3, 719 (1971).
[76] A. A. Lucas and M. Šunjić, Phys. Rev. Lett. 26, 229 (1971).
[77] V. Roundy and D. L. Mills, Phys. Rev. B5, 1347 (1972).
[78] E. Evans and D. L. Mills, ibid., p. 4126.
[79] H. Ibach, Phys. Rev. Lett. 27, 253 (1971).
[80] E. Evans and D. L. Mills, Phys. Rev. B7, 853 (1973).
[81] E. Evans and D. L. Mills, Sol. State Comm. 11, 1093 (1972).
[82] J. D. Axe and G. D. Pettit, Phys. Rev. 151, 676 (1966).
[83] V. V. Bryksin, Yu. M. Gerbshteĭn, and D. N. Mirlin, Fiz. Tverd. Tela 13, 1603 (1971) [Sov. Phys.-Solid State 13, 1342 (1972)] Sol. State Comm. 9, 669 (1971).
[84] T. P. Martin, ibid., p. 623.
[85] M. I. Abaev, V. N. Bogomolov, V. V. Bryksin, and N. A. Klushin, Fiz. Tverd. Tela 13, 1578 (1971) [Sov. Phys.-Solid State 13, 1280 (1971)].
[86] T. P. Martin, Phys. Rev. B1, 3480 (1970).
[87] R. Ruppin, ibid. B3, 4422 (1971).
[88] R. A. Cowley, Modern Solid State Physics, v. 2. Phonons and Their Interactions, N. Y.-L., Gordon and Breach, 1970.
[89] F. Placido and K. Hisano, Phys. Stat. Sol. b55, 113 (1973).
[90] L. Genzel and T. P. Martin, ibid. b51, 91 (1972).
[91] J. T. Luxon, D. J. Montgomery, and R. Summit, Phys. Rev. 188, 1345 (1969).
[92] H. G. Hafele, Ann. d. Phys. (Lpz.) 10, 321 (1963).
[93] J. T. Luxon, D. J. Montgomery, and R. Summit, J. Appl. Phys. 41, 2303 (1970).
[94] R. Kälin, H. P. Baltes, and F. K. Kneubühl, Sol. State Comm. 8, 1496 (1970); Helv. Phys. Acta 43, 487 (1970).
[95] J. Pastrňák J. and K. Vedam, Phys. Stat. Sol. a3, 647 (1970); J. Pastrňák, ibid., p. 657.
[96] C. T. Walker and I. R. Nair, Phys. Rev. B5, 4101 (1972).
[97] T. S. Sun and A. Anderson, Spectr. Lett. 4, 377 (1971).
[98] J. F. Scott and T. S. Damen, Opt. Comm. 5, 410 (1972).
[99] S. P. Srivastava and R. D. Singh, Phys. Stat. Sol. b45, 99 (1971); J. Phys. C4, 47 (1971).
[100] R. Ruppin and R. Englman, in: Light Scattering Spectra of Solids, Ed. G. B. Wright, N. Y., Springer, 1969, p. 157.
[101] M. Born and E. Wolf, Principles of Optics, Pergamon, 1970 Russ. transl., Nauka, 1972, p. 72.
[102] a) A. Otto, Zs. Phys. 216, 398 (1968); b) R. Ruppin, Sol. State Comm. 8, 1129 (1970).
[103] N. J. Harrick, Internal Reflection Soectroscopy, Wiley, 1967.
[104] V. V. Bryksin, Yu. M. Gerbshteĭn, and D. N. Mirlin, Fiz. Tverd. Tela 14, 543 (1972) [Sov. Phys.-Solid State 14, 453 (1972)] Phys. Stat. Sol. b51, 901 (1972).
[105] N. Marshall and B. Fisher, Phys. Rev. Lett. 28, 811 (1972).
[106] A. S. Barker, Jr., ibid., p. 892.
[107] V. V. Bryksin, Yu. M. Gerbshteĭn, and D. N. Mirlin, Fiz. Tverd. Tela 14, 3368 (1972) [Sov. Phys.-Solid State 14, 2849 (1973)].
[108] O. A. Dubovskiĭ, Fiz. Tverd. Tela 12, 3054 (1970) [Sov. Phys.-Solid State 12, 2471 (1971)].
[109] V. N. Lyubimov and D. G. Sannikov, Fiz. Tverd. Tela

14, 675 (1972) [Sov. Phys.-Solid State 14, 575 (1972)].
[110] V. V. Bryksin, D. N. Mirlin, and I. I. Reshina, ZhETF Pis. Red. 16, 445 (1972) [JETP Lett. 16, 315 (1972)].Fiz. Tverd. Tela 15, 1118 (1973) [Sov. Phys.-Solid State 15, 760 (1973)].
[111] N. Marshall, B. Fisher, and H. J. Quesser, Phys. Rev. Lett. 27, 95 (1971).
[112] D. Beaglehole, ibid. 22, 708 (1969).
[113] M. I. Kheĭfets, Fiz. Tverd. Tela 7, 3485 (1965) [Sov. Phys.-Solid State 7, 2816 (1966)].
[114] K. W. Chiu and J. J. Quinn, Phys. Lett. A35, 469 (1971).
[115] R. F. Wallis and J. J. Brion, Sol. State Comm. 9, 2099 (1971).
[116] I. I. Reshina, Yu. M. Gerbshtein, and D. N. Mirlin, Fiz. Tverd. Tela 14, 1280 (1972) [Sov. Phys.-Solid State 14, 1104 (1972)].
[117] V. V. Bryxin, D. N. Mirlin, and I. I. Reshina, Sol. State Comm. 11, 695 (1972).
[118] W. E. Anderson, R. W. Alexander, and R. J. Bell, Phys. Rev. Lett. 27, 1057 (1971).
[119] B. B. Varga, Phys. Rev. A137, 1896 (1965).
[120] A. A. Mooradion and G. B. Wright, Phys. Rev. Lett. 16, 999 (1967).
[121] Yu. A. Romanov, Izv. vuzov (Radiofizika) 7, 242 (1964).
[122] A. Pinczuk and E. Burstein, Proc. of the 10th Intern. Conference on Physics of Semiconductors, USA, 1970, p. 727.
[123] Yu. A. Romanov, Zh. Eksp. Teor. Fiz. 47, 2119 (1964) [Sov. Phys.-JETP 20, 1424 (1965)].
[124] K. W. Chiu and J. J. Quinn, Phys. Rev. Lett. 29, 600 (1972).
[125] R. H. Ritchie, Progr. Theor. Phys. 24, 607 (1963).
[126] A. J. Bennett, Phys. Rev. B1, 203 (1970).
[127] P. A. Fedders, ibid. 153, 438 (1967).
[128] D. E. Beck, ibid. B4, 1555 (1971).
[129] D. E. Beck and V. Celli, Phys. Rev. Lett. 28, 1124 (1972).
[130] P. J. Feibelman, C. B. Duke, and A. Bagchi, Phys. Rev. B5, 2436 (1972).
[131] R. H. Ritchie and A. L. Marusak, Surface Sci. 4, 234 (1966).
[132] D. Wagner, Zs. Naturforsch. 21a, 634 (1966).
[133] R. Fuchs and K. L. Kliewer, Phys. Rev. B3, 2270 (1971).
[134] J. Harris and A. Griffin, Phys. Lett. A34, 51 (1971).
[135] F. Flores and F. Garcia-Moliner, Sol. State Comm. 11, 1295 (1972).
[136] C. J. Powell and J. B. Swan, Phys. Rev. 115, 869; 116, 81 (1959); 118, 640 (1960).
[137] W. Steinman, Phys. Rev. Lett. 5, 470 (1960); Zs. Phys. 163, 92 (1961).
[138] V. L. Ginzburg and I. M. Frank, J. Phys. USSR, 9, 363 (1945); I. M. Frank, Usp. Fiz. Nauk 87, 189 (1965) [Sov. Phys.-Usp. 8, 729 (1966)].
[139] H. Böersch, P. Dobberstein, D. Fritsche, and G. Sauerbrey, Zs. Phys. 187, 97 (1965).
[140] R. H. Ritchie, Phys. Lett. A27, 660 (1968).
[141] A. J. Braundmeier, M. W. Williams, E. T. Arakawa, and R. H. Ritchie, Phys. Rev. B5, 2754 (1972).
[142] A. Bagchi and C. B. Duke, ibid., p. 2784.
[143] C. B. Duke and V. Landman, ibid. B6, 2956, 2968.
[144] E. A. Stern, Phys. Rev. Lett. 19, 1321 (1967).
[145] P. A. Fedders, Phys. Rev. 165, 580 (1968); 181, 1053 (1969).
[146] R. E. Palmer and S. E. Schnatterly, ibid. B4, 2329 (1971).
[147] J. C. Endriz and W. E. Spicer, ibid., p. 4144.
[148] J. Bramburg and H. Raether, Phys. Rev. Lett. 15, 882 (1965).
[149] E. Kretschmann, Opt. Comm. 5, 331; 6, 185 (1972).
[150] J. C. Endriz and W. E. Spicer, Phys. Rev. B4, 4159 (1972).
[151] D. C. Tsui, Phys. Rev. Lett. 22, 293 (1969).
[152] E. N. Economou, Phys. Rev. B4, 4165 (1971).
[153] R. L. Ngai and E. N. Economou, ibid., p. 2132.
[154] A. I. Akhiezer, V. G. Bar'yakhtar, and S. V. Peletminskiĭ, Spinovye volny (Spin Waves), Nauka, 1967.
[155] T. Wolfram and R. E. de Wames, Phys. Rev. B1, 4358 (1970).
[156] L. N. Bulaevskii, Fiz. Tverd. Tela 12, 799 (1970) [Sov. Phys.-Solid State 12, 619 (1970)].
[157] T. Wolfram, R. E. de Wames, and E. A. Kraut, J. Vac. Sci. and Techn. 9, 685 (1972).
[158] R. F. Wallis, A. A. Maradudin, I. P. Ipatova, and A. A. Klochikhin, Sol. State Comm. 5, 89 (1966).
[159] B. N. Filippov, Fiz. Tverd. Tela 9, 1339 (1967) [Sov. Phys.-Solid State 9, 1048 (1967)].
[160] M. Sparks, Phys. Rev. B1, 4439 (1970).
[161] T. Wolfram and R. E. de Wames, ibid. B4, 3125 (1971).
[162] A. S. Selivanenko, Zh. Eksp. Teor. Fiz. 32, 75 (1957) [Sov. Phys.-JETP 5, 79 (1957)].
[163] S. I. Pekar, ibid. 33, 1022 (1957) [6, 785 (1958)].
[164] V. I. Sugakov, Fiz. Tverd. Tela 5, 2207 (1963) [Sov. Phys.-Solid State 5, 1607 (1964)].
[165] Yu. V. Konobeev, Fiz. Tverd. Tela 9, 349 (1967) [Sov. Phys.-Solid State 9, 264 (1967)].
[166] V. I. Sugakov, Opt. Spektrosk. 28, 695 (1970), Fiz. Tverd Tela 14, 1977 (1972) [Sov. Phys.-Solid State 14, 1711 (1973)].
[167] M. S. Brodin, S. V. Marisova, and S. A. Shturkhetskaya, Ukr. Fiz. Zh. 13, 353 (1968).
[168] E. Glockner and H. C. Wolf, Zs. Naturforsch. 24a, 943 (1969); M. S. Brodin, S. V. Marisova, and S. A. Shturkhetskaya, Opt. Spektrosk. 31, 749 (1971).
[169] M. I. Kaganov and I. A. Shklovskaya, Fiz. Tverd. Tela 8, 2789 (1967) [Sov. Phys.-Solid State 8, 2227 (1968)].
[170] J. D. Blenstein, Appl. Phys. Lett. 13, 412 (1968).
[171] Yu. V. Gulyaev, ZhETF Pis. Red. 9, 63 (1969) [JETP Lett. 9, 37 (1969)].
[172] V. I. Baibakov and V. N. Datsko, Fiz. Tverd. Tela 13, 3133 (1971) [Sov. Phys.-Solid State 13, 2637 (1972)].
[173] V. M. Agranovich, A. G. Mal'shukov, and M. A. Mekhtiev, Zh. Eksp. Teor. Fiz. 63, 2274 (1972) [Sov. Phys.-JETP 36, 1203 (1973)]. V. M. Agranovich, Fiz. Tverd. Tela 14, 3684 (1972) [Sov. Phys.-Solid State 14, 3085 (1973)].
[174] R. Fuchs, Phys. Lett. A43, 42 (1973).
[175] A. A. Maradudin and D. L. Mills, Phys. Rev. B7, 2787 (1973).
[176] G. S. Agarwal, D. N. Pattanayak, and E. Wolf, Phys. Rev. Lett. 27, 1022 (1971); Opt. Comm. 4, 255, 260 (1971); 6, 221 (1972); Phys. Lett. A40, 279 (1972); A. Stahl and H. Wolters, Zs. Phys. 255, 227 (1972); J. L. Birman, and J. J. Sein, Phys. Rev. B6, 2482 (1972); R. Zeyher, J. L. Birman, and W. Brenig, ibid. p. 4613, 4617; V. M. Agranovich and V. I. Yudson, Opt. Comm. 7, 121 (1973).
[177] S. Q. Wang and G. D. Mahan, Phys. Rev. B6, 4517 (1972).
[178] J. Sak, ibid., p. 2482.
[179] V. N. Bogomolov, V. V. Bryksin, A. A. Sitnikova, V. D. Tolmacheva, and L. Kh. Ém, Fiz. Tverd. Tela

15, 2346 (1973) [Sov. Phys.-Solid State 15, 1503 (1974)].
[180] J. Nahum and R. Ruppin, Phys. Stat. Sol. a16, 459 (1973).
[181] A. J. Hunt, T. R. Steyer, and D. R. Huffman, Surface Sci. 36, 454 (1973).
[182] R. Ruppin, ibid. 34, 20.
[183] R. G. Schlecht and H. K. Böckelmann, Phys. Rev. Lett. 31, 930 (1973).
[184] A. F. van Gelder, J. Holvast, J. H. M. Stoelinga, and P. Wyder, J. Phys. C5, 2757 (1972).
[185] A. S. Barker, Surface Sci. 34, 62 (1973); Proc. of the Intern. Conference on Polaritons, Taormina (Italy), Nuovo Cimento (in press).
[186] B. Fisher, N. Marschall, and H. Quiesser, Surface Sci. 34, 50 (1973).
[187] Yu. A. Pasechnik, O. V. Snitko, O. M. Getsko, and V. F. Romanenko, ZhETF Pis. Red. 17, 587 (1973)]. [JETP Lett. 17, 416 (1973)].
[188] D. J. Evans, S. Ushioda, and J. D. McMullen, Phys. Rev. Lett. 31, 369 (1973).
[189] D. L. Mills and A. A. Maradudin, ibid., p. 372.
[190] I. I. Reshina and V. M. Zolotarev, Fiz. Tverd. Tela 15, 3020 (1973) [Sov. Phys.-Solid State 15, 2012 (1974)]. N. J. Falge and A. Otto, Phys. Stat. Sol. b56, 523 (1973); A. Hartstein, E. Burstein, J. J. Brion, and R. V. Wallis, Sol. State Comm. 12, 1083 (1973).
[191] H. Lüth, Phys. Rev. Lett. 29, 1377 (1972).
[192] J. J. Brion, R. F. Wallis, A. Hartstein, and E. Burstein, Surface Sci. 34, 73 (1973).
[193] E. D. Palik, R. Kaplan, R. W. Cammon, H. Kaplan, J. J. Quinn, and R. F. Wallis, Phys. Lett. A45, 143 (1973).
[194] L. Genzel and T. P. Martin, Surf. Sciace 34, 33 (1973).
[195] K. H. Rieder, M. Ishigame, and L. Genzel, Phys. Rev. B6, 3804 (1972).

Translated by J. G. Adashko